Distribution of mesopelagic scattering layer (MSL) in relation to the physical environment in the Norwegian Sea

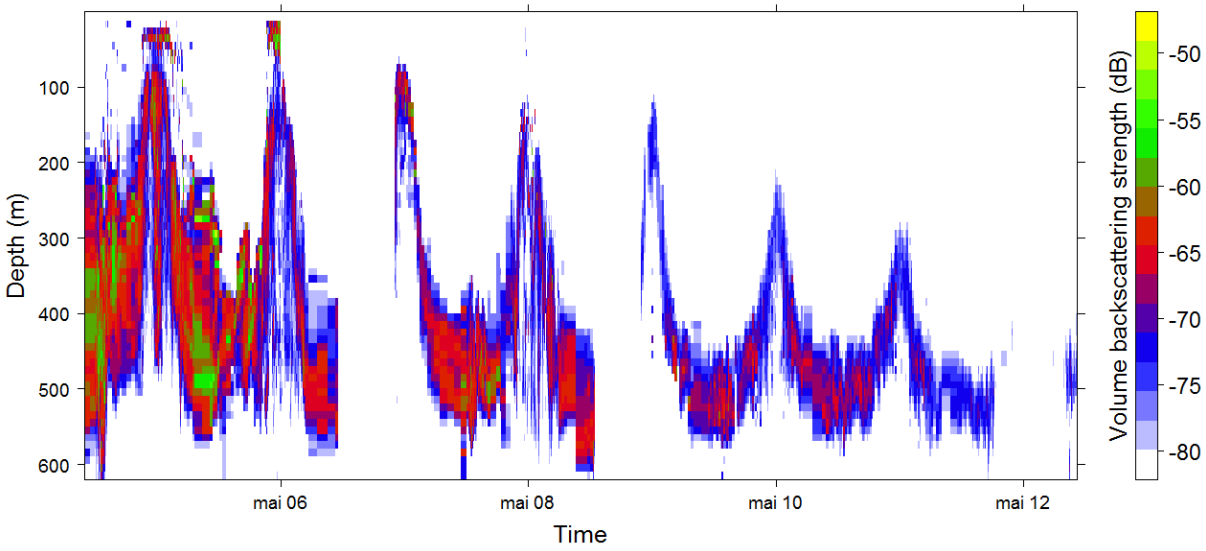

Masterthesis

Spring 2014

By Eirik Norheim

Supervisors: Professor Dag Lorents Aksnes, UIB & TEG, and Dr. Thor Aleksander Klevjer, IMR

University of Bergen

Institute of Biology

Master of Science: Program of Biodiversity, Evolution and Ecology

Table of contents

Abstract

Mesopelagic fish are considered a major group of fishes in the global oceans and are typically observed in the water as acoustic scattering layers. Their biomass has recently been suggested to be severely underestimated, and they might be a major component in the transport of organic material in the water column.

I observed the mesopelagic scattering layer (MSL) in the Norwegian Sea and in the Icelandic Sea. I investigated which physical forces might affect diel-vertical migration (DVM) behavior of the MSL. These factors included light, temperature, oxygen and salinity. On the basis of some simplifying assumptions I have approximated the biomass of the MSL and discussed its potential role in the Norwegian Sea ecosystem.

My results suggest that the changes in the mean depth (Z_m) of the MSL was consistent with DVM. The variation in Z_m correlated with the variation in surface irradiance. The ambient light of the Z_m showed far less variation than the surface irradiance. These observations suggest that DVM of the MSL emerges from a tendency of the organisms of the MSL to stay within a certain light regime which appears consistent with the antipredation window hypothesis. Other physical factors did not seem to affect the DVM patterns.

Benthosema glaciale were present in the trawl catches and might have been an important component of the MSL. The density, and thereby the approximated biomass, of the MSL decreased along the track concurrently with a decrease in temperature. The approximated biomass appeared to be larger than indicated in previous studies based on net sampling. My estimate, however, is subject to large uncertainties which include species composition, target strength and weight values.

1.0 Introduction

The mesopelagic zone, between 200 and 1000 m depths (Kaiser et al., 2005), includes a variety of organisms across the animalia kingdom (Gjosaeter and Kawaguchi, 1980, Shea and Vecchione, 2010, Siokou et al., 2013). Many mesopelagic fishes have been associated with the deep-scattering layer (DSL). They are known to be feeding on zooplankton (Kaartvedt, 2000, Bagoien et al., 2001, Eiane et al., 2002, Dypvik et al., 2012a, Pepin, 2013) and preyed upon by predators, usually visually predators (Hopkins et al., 1996, Marchal and Lebourges, 1996). These predators include epipelagic fishes (Marchal and Lebourges, 1996), marine mammals (Pauly et al., 1998) and seabirds (Barrett, 2002).

Mesopelagic fishes often engage in diel-vertical migration (Barham, 1966, Balino and Aksnes, 1993), where they migrate and distribute vertically in the water column. This migrational pattern were observed early by Barham (1966) and later linked to foraging behaviour (Isaacs et al., 1974). This vertical migration has been seen to differ seasonally and diurnally in some regions (Staby et al., 2011). Mesopelagic fish have also been observed conducting Inverse DVM (IDVM) (Dypvik et al., 2012a), non-migration (Staby et al. 2013), and other migratory behaviors like midnight sinking (Staby et al., 2011). Many of the studies concerning the migration behavior of mesopelagic fish have been done in fjords (Kaartvedt et al., 2008, Kaartvedt et al., 2009, Staby et al., 2011, Staby and Aksnes, 2011, Dypvik et al., 2012b).
There are several factors that have been suggested to influence DVM. Ultimate factors such as bioenergetics (Brett, 1971), foraging opportunity (Janssen and Brandt, 1980), and anti-predation behavior (Eggers, 1978) have been the primary hypotheses (Clark and Levy, 1988). Several studies have brought up the importance of light for DVM, mostly in light of predation risk (Clark and Levy, 1988, Cohen and Forward, 2009). The antipredation window hypothesis is perhaps the most complete of these hypotheses. It combines the ultimate factors of forage opportunities and predator risk and proximate factor of light, in sense of optical visual properties (Clark and Levy, 1988). Water layers with low oxygen contents might act as anti-predation refugias for mesopelagic organism, and thereby facilitate DVM (Bianchi et al., 2013).
There have been studies attempting to estimate biomass of mesopelagic fishes in local areas (McClatchie and Dunford, 2003, Sutton et al., 2008, Lara-Lopez et al., 2012). Gjosaeter and

Kawaguchi (1980), estimated mesopelagic fish biomass on a global scale. They presented an estimate of 945 million tons (wet weight), which were slightly corrected to 999 million tons by Lam & Pauly, 2005. These estimates were mainly based on trawl catches. Use of acoustic equipment has uncovered potential bias in the trawl estimates (Kaartvedt et al., 2012). Gjosaeter and Kawaguchi (1980) suggested in their study that trawl avoidance behaviour might cause underestimation. Kaartvedt et al. (2012) supported this and presented local biomass estimates in a fjord. The acoustic biomass estimates 1-2 order of magnitude higher than the trawl estimates. Irigoien et al. (2014) presented global estimates that were an order of magnitude higher than the estimate from Gjøsæter and Kawaguchi.

The influence mesopelagic fishes have on marine ecosystems would obviously depend on their actual biomass. Several studies suggest that mesopelagic fishes are an important consumer of zooplankton (Hopkins et al., 1996, Bagoien et al., 2001), and *Benthosema glaciale* is known to severely affect *Calanus* mortality and abundance, at least in a fjord system (Bagoien et al., 2001). How this group of fish may affect zooplankton in the Norwegian Sea is unclear. The influence of mesopelagic fishes in the food-web and oceanic ecosystems has been discussed over the last decades. Gjosaeter and Kawaguchi (1980), argued for their importance already then, but acknowledged the lack of data concerning their ecology. This in contrast with other more studied groups, such as zooplankton (Hays, 2003) and epipelagic fish (Palomera et al., 2007). The role of mesopelagic fishes in the oceanic carbon cycle may be larger than previously thought (del Giorgio and Duarte, 2002, Wilson et al., 2009, Irigoien et al., 2014). Hernandez-Leon et al. (2010), argued that migrant predators may be an important factor in the biological pump.

There are some studies that have shown presence of the mesopelagic fishes *Benthosema glaciale* (Glacier lanternfish), *Maurolicus muelleri* (Pearlside), and *Arctozenus risso* in the Norwegian Sea (Torgersen et al., 1997, Dalpadado et al., 1998, Dale et al., 1999) (Gjosaeter, 1981). *B. glaciale* belong to the myctophids, which are considered to be the most widespread mesopelagic fishes (Catul et al., 2011) both taxonomically and geographically. Gjosaeter (1981), studied the life histories of *B. glaciale*, focusing on age, growth, fecundity and reproduction in the Norwegian shelf. Kaartvedt et al. (1998) found schooling behaviour

in mesopelagic fish in the Norwegian Sea. They ascribed the scattering layer to *Maurolicus muelleri*.

The aims of this study is to (1) observe the mesopelagic distribution patterns in the Norwegian Sea and the Icelandic Sea, specifically the diel-vertical migration patterns, and (2) to identify which physical factors may affect the distribution and behavior. I observed the spatio-temporal vertical distribution of a mesopelagic scattering layer (MSL) along a track from the Norwegian Sea, to the Icelandic Sea.

2.0 Methods

2.1 The sampling area

The data were sampled in the Norwegian Sea and the Icelandic Sea, along a transect with the research vessel G.O Sars. The sampling took place between the 4 th May and the 12th May 2013. It was a part of a large integrated scientific program, EURO-BASIN. The G.O Sars was set to survey from Bergen to Nuuk, and back again, over a period of 6 weeks, from 1 th May to the 14 th June 2013. The data used for this study were sampled in the first leg from Bergen, Norway, to Reykjavik, Iceland. The cruise followed a track across the Norwegian Sea into the Icelandic Sea (Figure 1).

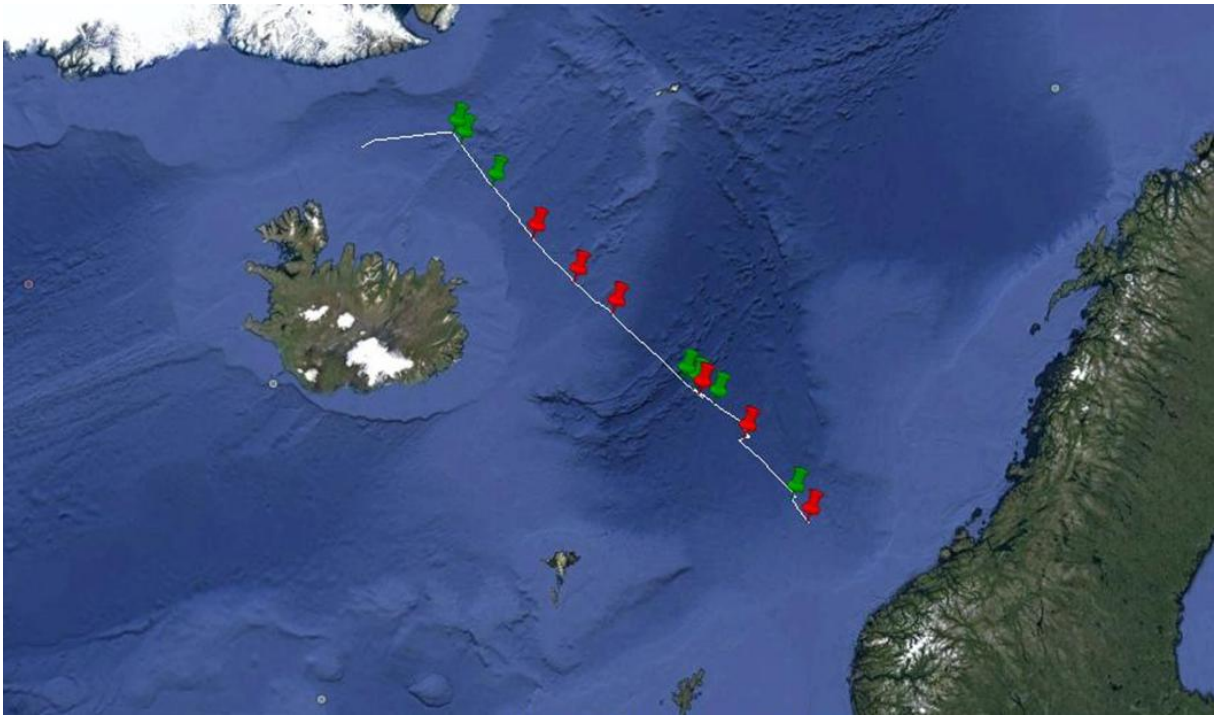

Figure 1. Map of the cruise track. Pin head symbols represent CTD stations (153-165) along the track. Starting in the eastern Norwegian Sea 4th May, and ending in the western Norwegian Sea/Icelandic Sea 12th May. Red pin head symbols represent CTD stations were underwater light was measured.

2.2 Hydrographical observations

The hydrographical data includes temperature, salinity, Sigma-t (σ_t), oxygen, and fluorescence. These measurements were acquired by the CTD (Conductivity, temperature and depth) water sampling package. The hydrographical data were sampled by lowering the CTD-package down the water column. Throughout the first leg, there are 13 CTD-stations (Table 1). The hydrographical variables were interpolated between the stations to create isoplot diagrams along the track. Mean values of the hydrographical variables, were calculated for every nautical mile in the upper 600 meters.

Table 1. Overview of the CTD stations.

Station	Date & Time	Latitude	Longitude	CTD Depth (m)	Depth (m) for measurement of underwater light	Underwater light
153	04.05.2013 10:24:23	63 45.81 N	2 45.81 E	1002	102.6	X
154	04.05.2013 17:45:57	64 7.75 N	1 7.75 E	155		
155	05.05.2013 7:49:11	65 3.33 N	3.33 W	2870	167.2	X
156	06.05.2013 01:06:52	65 34.15 N	2 34.15 W	503		
157	06.05.2013 05:07:38	65 45.86 N	3 45.86 W	3120		
158	07.05.2013 10:50:53	65 40.1 N	3 40.1 W	1002	186.7	X
159	07.05.2013 20:35:57	65 51.75 N	3 51.75 W	201		
160	08.05.2013 09:00:46	66 42.25 N	7 42.25 W	1000	220.8	X
161	09.05.2013 08:21:43	67 3.28 N	9 3.28 W	1000	231.4	X
162	10.05.2013 06:31:35	67 33.8 N	12 33.8 W	1000	230.8	X
163	11.05.2013 08:54:09	68 10.44 N	15 10.44 W	1350		
164	11.05.2013 20:37:02	68 39.39 N	17 39.39 W	502		
165	11.05.2013 22:59:52	68 47.65 N	18 47.65 W	1063		

2.3 Acoustic observations

The acoustic data were sampled using the calibrated EK60 Simrad echo sounder. There were 6 different frequencies in use: 18, 38, 70, 120, 200 and 333 kHz with 1 ms pulse duration. The acoustical data are presented as s_A values (Nautical area backscattering, nautical mile^2 m^{-2}) which are the average amount of sound backscattered from the water column. These s_A values are given for 1 nautical mile by 10 m vertical segments. Only the 38 kHz data were used in this study, a common frequency for observations on mesopelagic fishes (Kaartvedt et al., 2009, Irigoien et al., 2014). The data were scrutinized by IMR personnel during the survey, with the LSSS software (Large Scale Survey System). This procedure included removal of false sea bottoms, and assignments of the acoustic scattering into different classes based on target strength and other characteristics. I used the class of mesopelagic organisms and the total backscattering. I concentrated on the mesopelagic scattering layer (MSL). In the literature it has often been referred to as either the deep scattering layer (DSL) (Barham, 1966). The density of the MSL in the present study is given by the backscattering values (s_A) at 38 kHz. I will also present results for the total scattering, i.e. the sum of all groups. The time between was defined as night time. Day time was determined approximately between 05:00 - 21:00, 2 h after sunrise and 2 hours before sunset. The time between (21:00 - 05:00) was defined as night time.

2.3.1 Characterization of the Mesopelagic Scattering Layer (MSL)

The following characteristics of the mesopelagic scattering layer were calculated according to Dupont and Aksnes (2012): The depth integrated abundance (A) and the mean depth (Z_m) of the vertical distribution in

$$A = \sum_{j=1}^{n} \Delta z_j f_j \,, \qquad \text{Eq. 1}$$

n is the number of depth layers, Δz_j is the the specific sampled depth layer, and f_j is the density (i.e. the s_A value) of the MSL in Δz_j.

The mean depth of the MSL:

$$Z_m := \sum_{j=1}^{n} \frac{\Delta z_j f_j z_j}{A}, \quad \text{Eq. 2}$$

The quantity Z_S has unit meters and indicates the vertical extension of the vertical distribution. Thus, a small and a large Z_S indicate a narrow and a wide MSL respectively. The depth layer, Δz_j, was always 10 m.

2.3.2 Estimation of MSL biomass

I conducted a rough estimate of biomass (kg) of the MSL. To estimate biomass of the MSL, three factors is needed: (1) the Area Backscatter coefficient (s_a), (2) the backscattering cross-section (σ_{bs}), and (3) the average weight per individual ($\overline{kg}$). I also converted the s_A values to volume backscattering coefficient ($S_V, dB\ re\ 1m^{-1}$).

To compute the area backscattering coefficient, I converted s_A to s_a. This is the backscatter from 1 m^2 over the entire integrated depth which is 1000 m.

$$s_a = \frac{s_A}{4\pi 1852^2} \quad \text{Eq. 3}$$

Then we need the backscattering cross-section, σ_{bs}:

$$\sigma_{bs} = 10^{\frac{\overline{TS}}{10}} \quad \text{Eq. 4}$$

$\overline{TS}$ is the average target strength used from literature (Irigoien et al., 2014), in this case the average TS from *Benthosema glaciale,* which was -58.0 dB. Target strength from B. glaciale was used since it was the only mesopelagic fish present in the trawl hauls, and since it is one of the dominant species in the Norwegian Sea (Gjosaeter and Kawaguchi, 1980). Target strength is the measure of proportion of energy which is backscattered (Simmonds & Maclennan 2005).

σ_{bs} and s_a is necessary to determine the number of individuals for 1 m^2 per 1000 m (ρ_v).

$$\rho_v = \frac{s_a}{\sigma_{bs}} \quad \text{Eq. 5}$$

From literature I used an average weight for converting to biomass, kg wet weight per m^2 integrated over 1000 m ($\frac{kg}{m^2}$). Here I use an average weight measure from literature (Irigoien

et al., 2014), in this case the average weight ($\overline{kg}$) from *Benthosema glaciale*, which is 0.003 kg.

$$\frac{kg}{m^2} = \rho_v * \overline{kg} \quad \text{Eq. 6}$$

The volume backscattering coefficient ($S_V, dB\ re\ 1m^{-1}$) was calculated. The nautical area backscattering coefficient is divided on the ΔZ, the entire integrated depth of 1000 m

$$S_V = 10LOG(\frac{S_a}{\Delta Z}) \quad \text{Eq. 7}$$

2.4 Light measurements

The CTD water sampler package was equipped with a underwater PAR (photosynthetic active radiation) sensor. This sensor was not used in the present study due to technical problems. The PAR observations would give unreliable measurements at larger depths in the ocean. In contrast to monochromatic irradiance (i.e light on a narrow band), the PAR observations are the summed irradiance between 400 to 700 nm. Some wavelengths are absorbed more strongly than others (Kirk, 1983), and the attenuation would decrease with increased depth. By using PAR I would get different attenuation coefficients than if I used monochromatic irradiance. PAR was thereby not relevant for measurements. Instead I used the wavelength prevailing at the mesopelagic depths, which is around 500 nm (Figure 2). The ship was also equipped with an atmospheric PAR sensor located at deck that stored information on incoming irradiance for each 10 min.

Instead of the PAR sensor attached to the CTD a Trios RAMSES ACC hyperspectral radiometer was used for measurements of downwelling irradiance at the CTD stations. Atmospheric irradiance was measured through the entire survey with 5 minute intervals, except when underwater irradiance was measured. Due to lack of cabling between the upper and the lower deck at the ship the atmospheric sensor had to be disconnected when the underwater measurements were taken. Therefore simultaneous measurements of both atmospheric – and underwater irradiance were not available with the radiometer. This resulted in some uncertainties for calculation of the attenuation coefficient, since changes in atmospheric light (such as increased sky cover) during the underwater measurements could not be accounted for properly. The PAR sensor on deck however, was measuring data continuously,

with an interval of 10 min. This gave some guidance whether irradiance changed during the underwater measurements (See appendix for more detail). Underwater light measurements could not be taken at all CTD stations due to rough weather conditions and a total of 6 underwater light stations were obtained during leg 1.

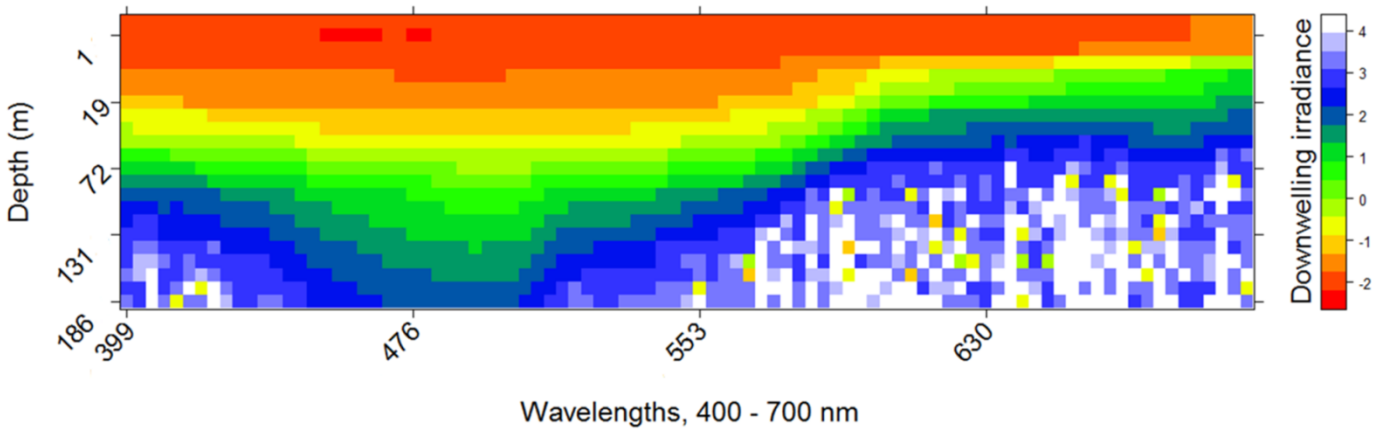

Figure 2. Downwelling irradiance as a function of wavelength and depth (m). Unit of irradiance is mW $m^{-2}nm^{-1}$ at 500 nm and is given as colour codes in log scale. NA-values are represented in white.

2.5 Calculation of the light attenuation coefficient

The attenuation coefficient for downwelling irradiance was estimated at the 6 stations from the underwater measurements by using regression analysis. I used the measurements at 500 nm in the electromagnetic spectrum, since it penetrates deepest in the water column (Figure 2.).

The regression equation was obtained from the equation for the attenuation of downwelling irradiance with depth:

$$E_d(z) = E_d(0)\ exp^{-K_d z} \qquad \text{Eq. 8}$$

Where $E_d(0)$ and $E_d(z)$ are the downwelling irradiance (at 500 nm) just below the sea surface and at depth z respectively, and K_d is the attenuation coefficient for the downwelling irradiance at 500 nm.

On logarithmic form:

$$\ln E_d(z) = \ln E_d(0) - K_d(z)\ z \qquad \text{Eq. 9}$$

Where ln $E_d(0)$ is the intercept and K_d is the slope of the linear regression equation. If the logarithmic transformed observations of E_d shows a linear decrease down the water column, the estimated slope of this line corresponds to the light attenuation coefficient. There were at times necessary to separate the downwelling irradiance measurements into two groups denoted as the upper layer Z_1 and lower layer Z_2 due to attenuation coefficient changing with depth (See appendix for more detail).

Since measurements of atmospheric PAR varied under some of the underwater measurements (See appendix for more detail), $E_d(0)$ varied accordingly. To determine the effect fluctuations in atmospheric light might have had on the uncertainty on the estimated light attenuation, I rearranged Eq. 9. The effect of $E_d(0)$ fluctuations will be reflected in the variation of the $K_d(z)$.

$$K_d(z) = \frac{-\ln\left(\frac{E_d(z)}{E_d(0)}\right)}{z} \qquad \text{Eq. 10}$$

The largest variation in $K_d(z)$ as a result of variation in $E_d(0)$ was 8 % at station 153. It ranged between 0.25 and 4.8 % at the other stations. See appendix for more detail.

2.6 Calculation of ambient irradiance at Z_m

To determine the underwater downwelling irradiance along the cruise track I Interpolated the estimated attenuation coefficients between stations. Downwelling irradiance was then calculated with Eq. 8. In some cases the attenuation coefficient of the upper layer was different from that of the lower layer, and the following expression was used.

$$E_d(z) = E_d(0)\, exp^{-K_{d1}Z_1} * exp^{-K_{d2}Z_2} \qquad \text{Eq. 11}$$

Where Z_1represent the upper layer, while Z_2 represent the lower layer, and K_{d1} and K_{d2} are attenuation coefficients of the two layers. $E_d(0)$ represents here the continuously measured atmospheric light.

2.7 Comparison of acoustics and light measurements

Linear regression analysis was conducted on the acoustic data, both MSL Z_m and total backscatter against log transformed surface irradiance. This was necessary since surface

irradiance varied from 0.0005 to over 1400 mW $m^{-2}nm^{-1}$ at 500 nm. I calculated the ambient light irradiance at Z_m for the entire leg. Downwelling irradiance was measured down to around 230 meters at the deepest station (see Table. 2). Therefore downwelling irradiance was extrapolated deeper than this depth with the assumption that the attenuation coefficient was constant.

2.8 Biological catches

Biological catches were obtained with the Harstad trawl and macrozooplancton trawl. The data is based on catches from 4 Harstad trawl hauls and 8 Macrozooplankton hauls. The Macrozooplankton trawl had an opening size of 6 X 6 meters, and the net had a mesh of equal size (3mm) from trawl opening to cod end. The Harstad trawl had an opening of 400 m^2. Mesopelagic fishes were all measured by length and a smaller subset by weight. The subset measured by weight came from one haul. Catches from the macrozooplankton trawl were measured in wet weight. The sampling capacity was severely reduced due to time constraints and technical problems onboard. The multisampler on the Macrozooplankton trawl did not function properly. It was originally supposed to sample independently at several depths, but all the samples were stored in the last net, making it impossible to distinguish depths.

2.9 Data Analysis

The statistical package R i386 3.0.2 and Microsoft Office Excel 2007 were used to prepare, plot and analyze the data in the present study. Google Earth was used to create a map over the survey area.

3.0 Results

3.1 Hydrographical observations

Sigma-t (σ_t) is determined by temperature and salinity (Kaiser et al., 2005). Water with high salinity (PSU) and low temperature (˚C) will be most dense and vice versa. σ_t increased along the track, from 27.5 to 28. The water column became more stratified (Figure 3), with σ_t ranging from 27.5 - 28.0 early in the survey, to 27.8 - 28.0 in the end. The temperature decreased in the upper 600 meters along the leg, from 6 -7 ˚C in the beginning at the east Norwegian Sea, down to 0-1 ˚C in the west, i.e Icelandic Sea. Salinity (PSU) decreased in the upper 600 meters, from 35.3 to 34.6 PSU. Oxygen levels (ml/l) increased from 6.2 to 7.8 ml/l in the upper 600 meters. Fluorescence both decreased and increased along the track, fluctuating from 0.2 to 0.8 mg chl m^{-3} in the upper 150-200 meters. Figure 4 shows the vertical profile of all the physical factors down to 2800 m at station 155.

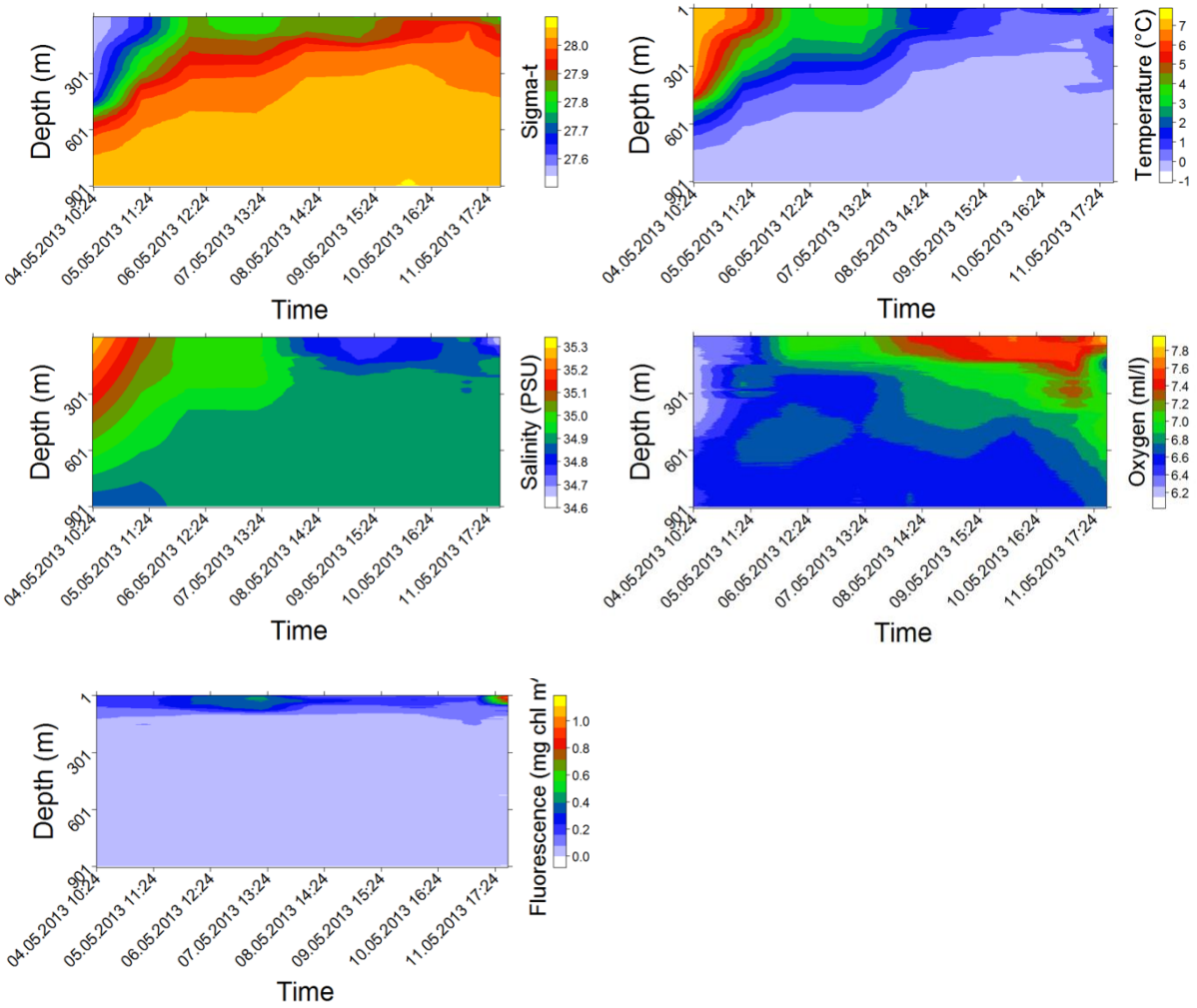

Figure 3. Vertical distribution of hydrographical factors interpolated along the cruise track. σ_t (upper left), temperature (˚C, upper right), salinity (PSU, middle left), oxygen (ml/l, middle right) and fluorescence (mg chl m^{-3}, lower left) and across the leg. The track begins in the eastern Norwegian Sea at 4th May and ends at the Icelandic Sea at 12th May.

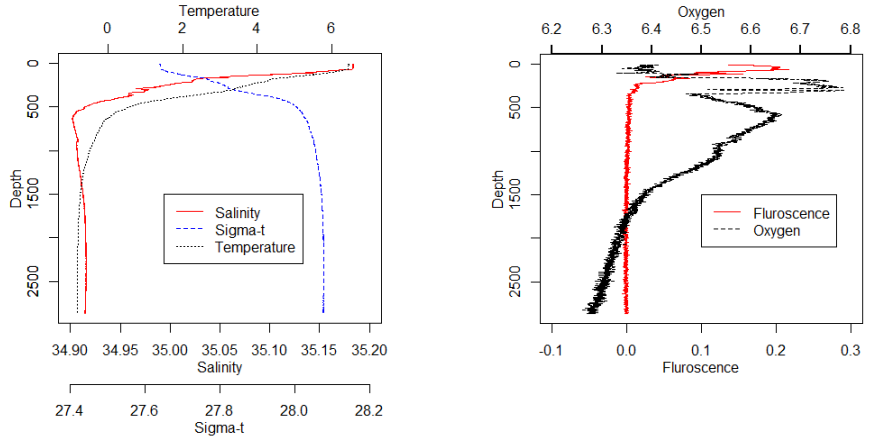

Figure 4. Vertical profiles of temperature (˚C), oxygen (ml/l), salinity (PSU), σ_t and fluorescence (mg chl m^{-3}) down to 2800 meters at station 155.

3.2 Spatial and temporal variation in surface irradiance

The measurements of surface irradiance showed diel variations of 3 to 6 orders of magnitude during the leg (Figure 5). The surface irradiance are highest during the day and lowest during night. The irradiance at night time increased by 2 - 3 orders of magnitude along the track. The daytime irradiance on the other hand, decreased by nearly 1 order of magnitude along the track.

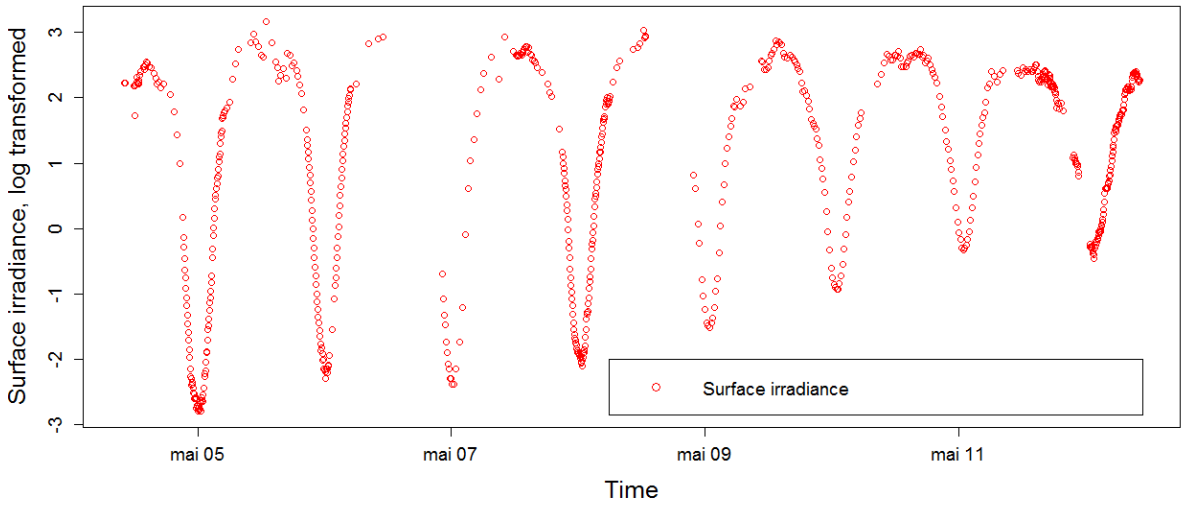

Figure 5. Surface irradiance (mW $m^{-2}nm^{-1}$ at 500 nm), log transformed, during the leg. The track begins in the eastern Norwegian Sea at 4th May and ends at the Icelandic Sea at 12th May.

3.2.2 Calculation of the attenuation coefficient for downwelling irradiance

The estimated attenuation coefficients are given in Table 2. Details are presented in the Appendix. The attenuation coefficient increased from 0.0495 at station 153 to 0.0647 at station 158, and then decreased to 0.0470 at station 162.

Table 2. Calculated light attenuation coefficients for 500 nm. Z_1 and Z_2 represent the upper and lower layer. The table also contain the potential errors in K due to change in atmospheric light during the measurements.

Station	Max depth (m)	Number of measurements	Attenuation Coefficient	R^2	Potential errors in K due to change in atmospheric light
153	102.6				
0 – 103 m		8	0.0495 ± 0.0015	0.9989	8 %
155	167.2				0.4 %
Z_1 (0 – 90 m)		6	0.0553± 0.0015	0.996	
Z_2 (90–170 m)		14	0.0464 ± 0.0006	0.997	
158	186.7				3.8 %
Z_1 (0 – 90 m)		13	0.0674± 0.0019	0.998	
Z_2 (90 – 190 m)		9	0.0387± 0.0012	0.9985	
160	220.8				2.2 %
Z_1 (0 – 110 m)		5	0.0541 ± 0.0033	0.9957	
Z_2 (110 – 220 m)		4	0.0357 ± 0.0010	0.9987	
161	231.4				0.25 %
Z_1 (0 – 135 m)		10	0.0427 ± 0.0012	0.9986	
Z_2 (135 – 230 m)		9	0.0367 ± 0.0016	0.9972	
162	230.8				4.8 %
Z_1 (0 – 100 m)		11	0.0470 ± 0.0011	0.9987	
Z_2 (100 – 230 m)		10	0.0369 ± 0.0015	0.9969	

3.3 Acoustic observations

The MSL is located in the upper 600 meters (Figure 6, 7). During the day the MSL is located between 300 and 600 m, while during night it was located between 50 and 300 m. During dusk and dawn, the MSL was located between these depths. This is consistent with diel vertical migration (DVM) patterns, with ascent during dusk and descent during dawn. The MSL became deeper along the track, descending deeper during dawn and ascending deeper during dusk. The Nautical area scattering coefficient (s_A) of the MSL are more dense in the first part of the track, and then decreases towards the end (Figure 6, Table 3). It decreased by 1-2 orders of magnitude. The s_A values for the MSL ranged from 1.16 – 54486 $m^2/n.mi^2$. The Total backscatter is seen in Figure 8. Combined Total backscatter (s_A) were between 1.05 and 3.9 times higher than mesopelagic scattering across the track. (Table 3).

The MSL biomass estimate which were denoted as $\frac{kg}{m^2}$ of the upper 1000 m, varied between 0.00005 and 2.4 $\frac{kg}{m^2}$, with a mean biomass of 0.067 $\frac{kg}{m^2}$ ± 0.062. The biomass decreased along the track (Table 4), by 1 order of magnitude. The MSL biomass was between 1.2 and 7 times higher during day than night. The mean s_A at day- and night time and throughout the day are located in Table 5.

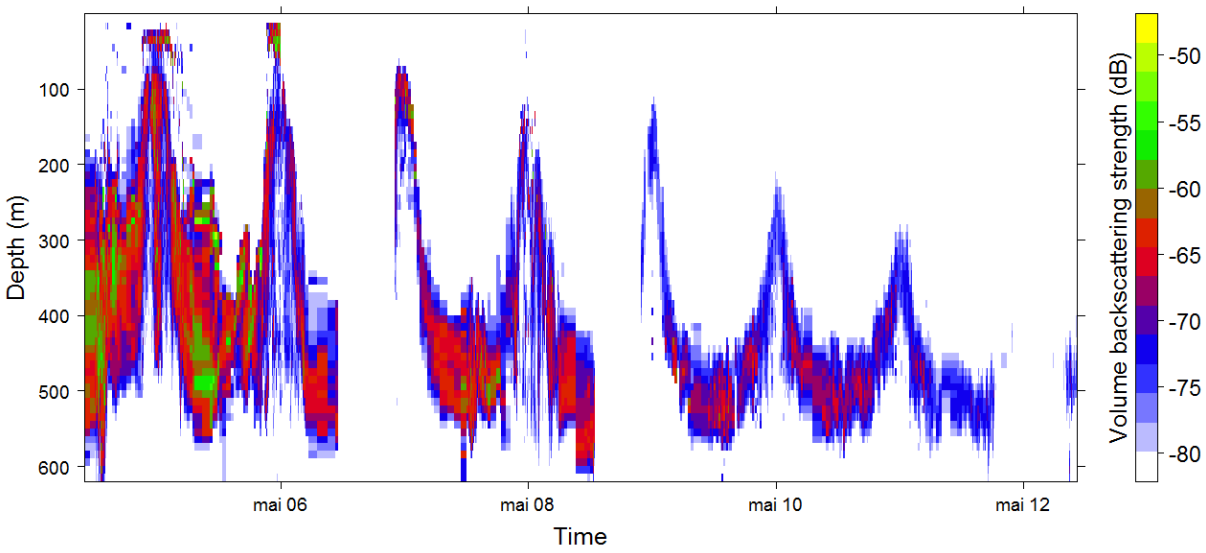

Figure 6. Mesopelagic volume backscattering strength (S_V, dB re m^{-1}) from 4th to 12th May. The two vertical white bands represent lack of observations. The track begins in the eastern Norwegian Sea at 4th May and ends at the Icelandic Sea at 12th May.

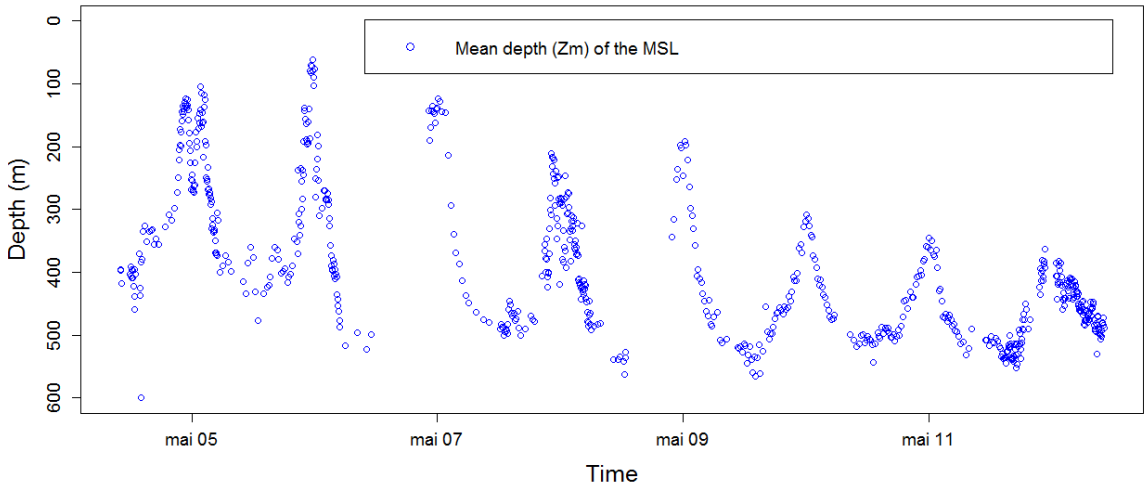

Figure 7. Mean depth (Zm in Eq. 1) of the mesopelagic scattering layer from 4th to 12th May. The track begins in the eastern Norwegian Sea at 4th May and ends at the Icelandic Sea at 12th May.

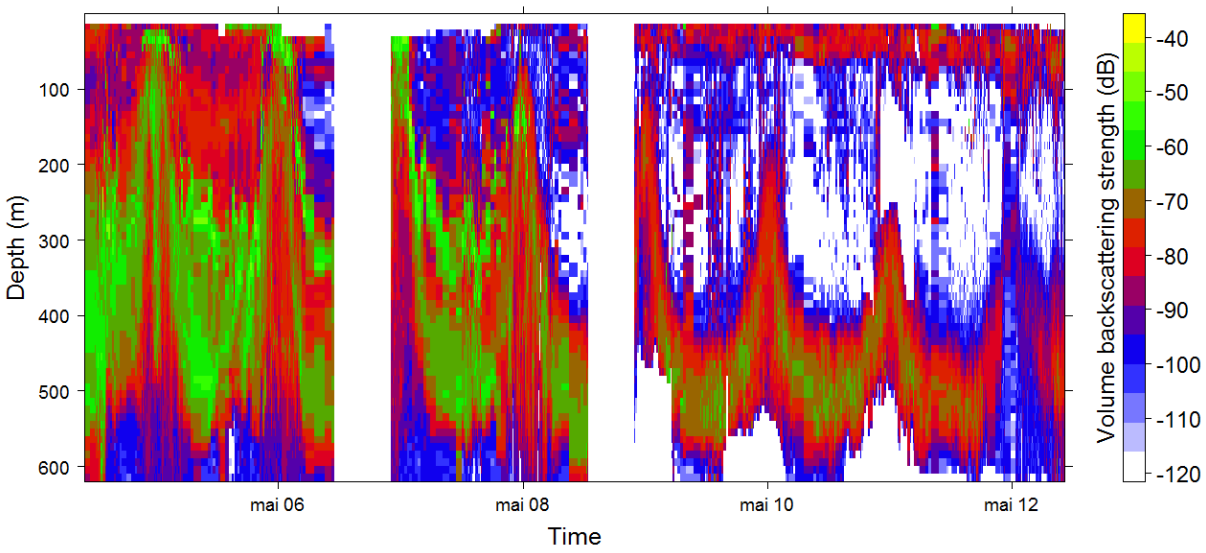

Figure 8. Total volume backscattering strength (S_V, dB re m^{-1}) from 4th to 12th May. The two vertical white bands represent lack of observations. The track begins in the eastern Norwegian Sea at 4th May and ends at the Icelandic Sea at 12th May.

Table 3. Overview of daily mean s_A values for 1 nautical mile, for mesopelagic backscatter and total backscatter, with the standard deviation of the mean for each sample.

Day	Mesopelagic s_A $(m^2/\,n.mi^2)$	Total s_A $(m^2/\,n.mi^2)$
4th	5846 ± 3522	7466 ±4718
5th	3519 ± 1034	5299 ±1819
6th	1163 ± 362	4513 ±1421
7th	1364 ± 471	5129 ±2101
8th	1063 ± 396	2422 ±2764
9th	490 ± 154	542 ± 173
10th	464 ± 88	491 ± 90
11th	184 ± 70	218 ± 72

Table 4 Mean biomass (kg/m^2 of the upper 1000 m) of the MSL, for each day from 4th to 12th May, with the standard deviation of the mean for each sample. Mean value at daytime, night time and entire day combined. Day and night was defined in the time frames 05:00 – 21:00 and 21:00 – 05:00 respectively. 0.055 ± 0.010

Day	Mean biomass at day (kg/ m^2)	Mean biomass at night (kg/ m^2)	Mean diel biomass (kg/ m^2)
4th	0.382 ± 0.194	0.138 ±0.036	0.260 ± 0.154
5th	0.201 ±0.063	0.079 ±0.024	0.140 ± 0.045
6th	0.055 ± 0.010	0.044 ±0.018	0.050 ± 0.015
7th	0.081 ±0.024	0.048 ±0.016	0.064 ± 0.020
8th	0.045 ±0.010	0.014 ±0.006	0.030 ± 0.017
9th	0.025 ±0.006	0.016 ±0.004	0.021 ± 0.006
10th	0.021 ±0.002	0.016 ±0.004	0.018 ± 0.003
11th	0.007 ±0.001	0.001 ±0.0001	0.004 ± 0.003

Table 5. Mean Mesopelagic s_A ($m^2/\ n.mi^2$) of the MSL, for each day from 4th to 11th May, with the standard deviation of the mean for each sample. Mean value at daytime, night time and entire day combined. Day and night was defined in the time frames 05:00 – 21:00 and 21:00 – 05:00 respectively.

Days	Mean day time Mesopelagic s_A ($m^2/\ n.mi^2$)	Mean night time Mesopelagic s_A ($m^2/\ n.mi^2$)	Mean Mesopelagic s_A ($m^2/\ n.mi^2$) for entire day.
4th	8713 ± 4435	3157 ± 832	5846 ± 3522
5th	4579 ± 1437	1796 ± 559	3519 ± 1034
6th	1271 ± 229	1020 ± 417	1163 ± 362
7th	1847 ± 568	1095 ± 375	1364 ± 471
8th	1030 ± 239	335 ± 145	1063 ± 396
9th	580 ±155	379 ± 101	490 ± 154
10th	490 ± 65	367 ± 99	464 ± 88
11th	168 ± 39	8 ±4	184 ± 70

3.4 Comparison of irradiance and acoustics

3.4.1 Surface irradiance and MSL Z_m

There is an inverse relationship between surface irradiance and MSL Z_m . At low illumination, the MSL Z_m was shallowest and at high illumination the MSL Z_m was deepest (Figure 9). A linear regression analysis was conducted between the MSL Z_m and the log surface irradiance. It showed a significant negative correlation between the two variables

(Figure. 10), with an R^2= 0.69. A similar analysis was made for the mean depth of the total backscatter and surface irradiance (Figure 11). The coefficient of determination for the total backscatter, R^2(0.51), was lower than for the MSL. The nigh time depth was correlated with surface irradiance (R^2= 0.69) (Figure 12). The MSL Z_m depths at night were distributed deeper with increased surface irradiance at night.

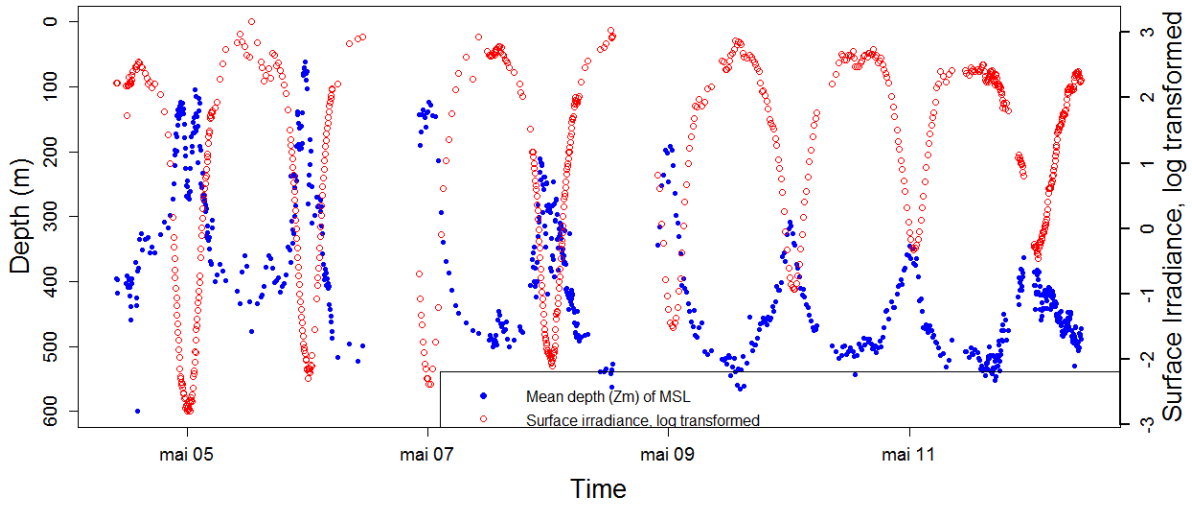

Figure. 9. Timeseries of the mean depth (blue, Z_m(Eq. 1)) of the mesopelagic scattering layer and observed surface irradiance (red, mW $m^{-2}nm^{-1}$ at 500 nm), log transformed, during the investigated period from 4th to 12th May. The track begins in the eastern Norwegian Sea at 4th May and ends at the Icelandic Sea at 12th May.

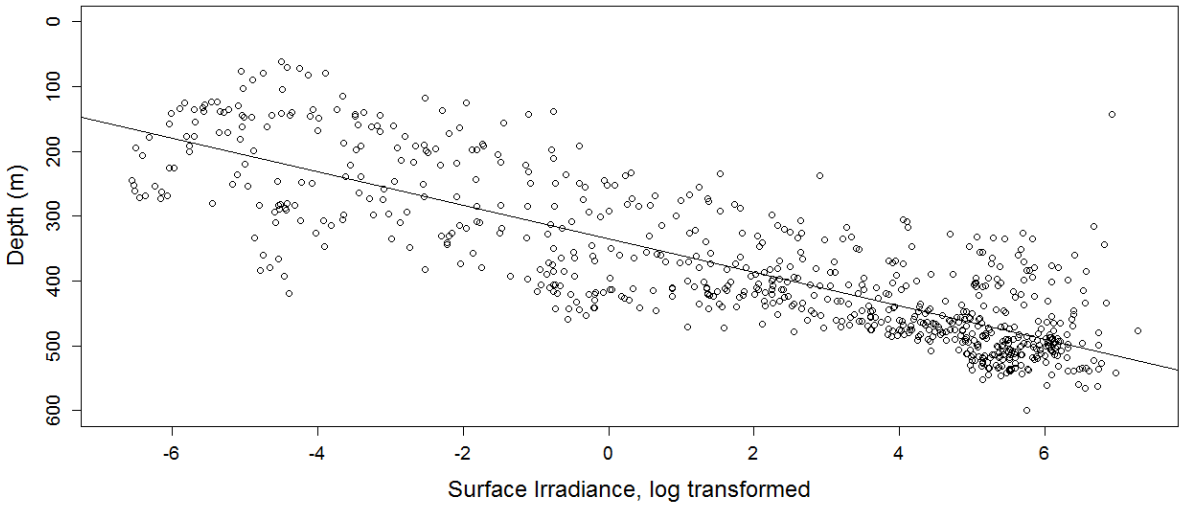

Figure 10. Linear regression between the mean depth (Z_m, Eq. 1) of the mesopelagic scattering layer and surface irradiance (mW $m^{-2}nm^{-1}$ at 500 nm), log transformed. (Z_m = -25.9*log10(E) + 335.1, R^2 = 0.69, Pr(>|t|) <2x10^{-16}, n = 730

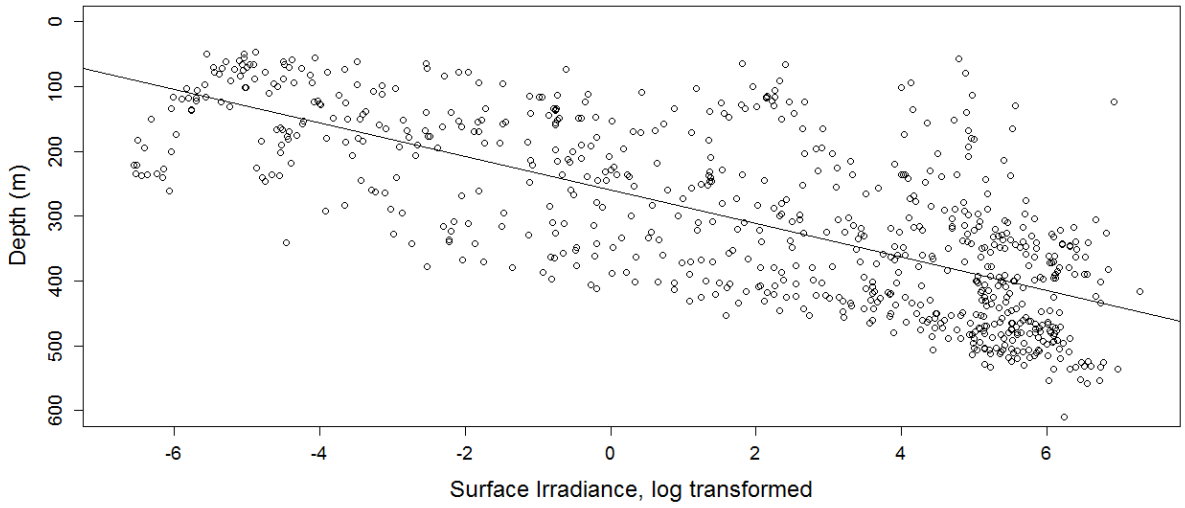

Figure 11. Linear regression between the mean depth (Z_m, Eq. 1) of total scattering , and surface irradiance (mW $m^{-2}nm^{-1}$ at 500 nm), log transformed.(Z_m = -25.9*log10(E)+ 259.2, R2 = 0.51, Pr(>|t|) <2 x 10^{-16} , n= 730)

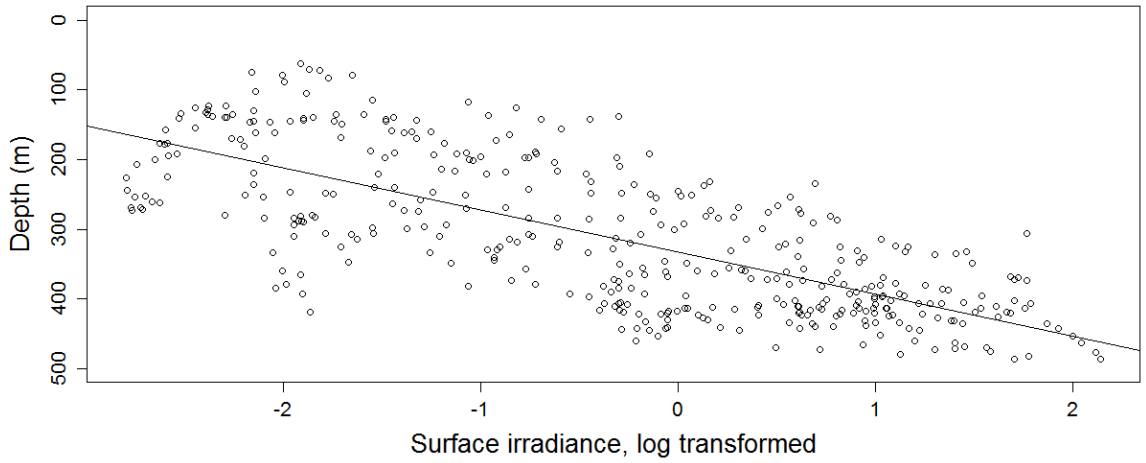

Figure 12. Linear regression between the mean depth at night time (Z_m, Eq. 1) of MSL , and surface irradiance(mW $m^{-2}nm^{-1}$ at 500 nm), log transformed. (Z_m = - 60.4*log10(E)+ 333.0, R2 = 0.54, Pr(>|t|) <2 x 10^{-16} , n= 396)

3.4.2 Calculated ambient irradiance at Z_m

The ambient irradiance at Z_m ranged between 10^{-6} and 10^{-9} mW $m^{-2}nm^{-1}$ at 500 nm (Figure 13). The geometrical mean was about 10^{-7} mW $m^{-2}nm^{-1}$ at 500 nm. A scatterplot of ambient irradiance at Z_m and the MSL Z_m as a function of time is shown in Figure 14.

From 4th to 12th May the ambient irradiance at Z_m showed less variation than the surface irradiance.

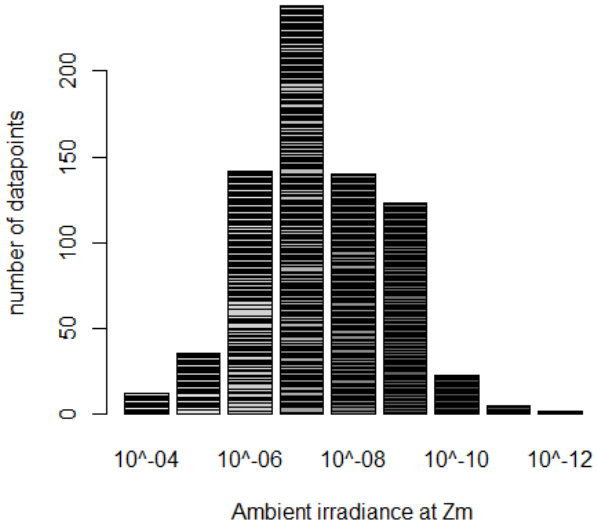

Figure 13 Distribution of ambient irradiance values at Z_m (mW $m^{-2}nm^{-1}$ at 500 nm).

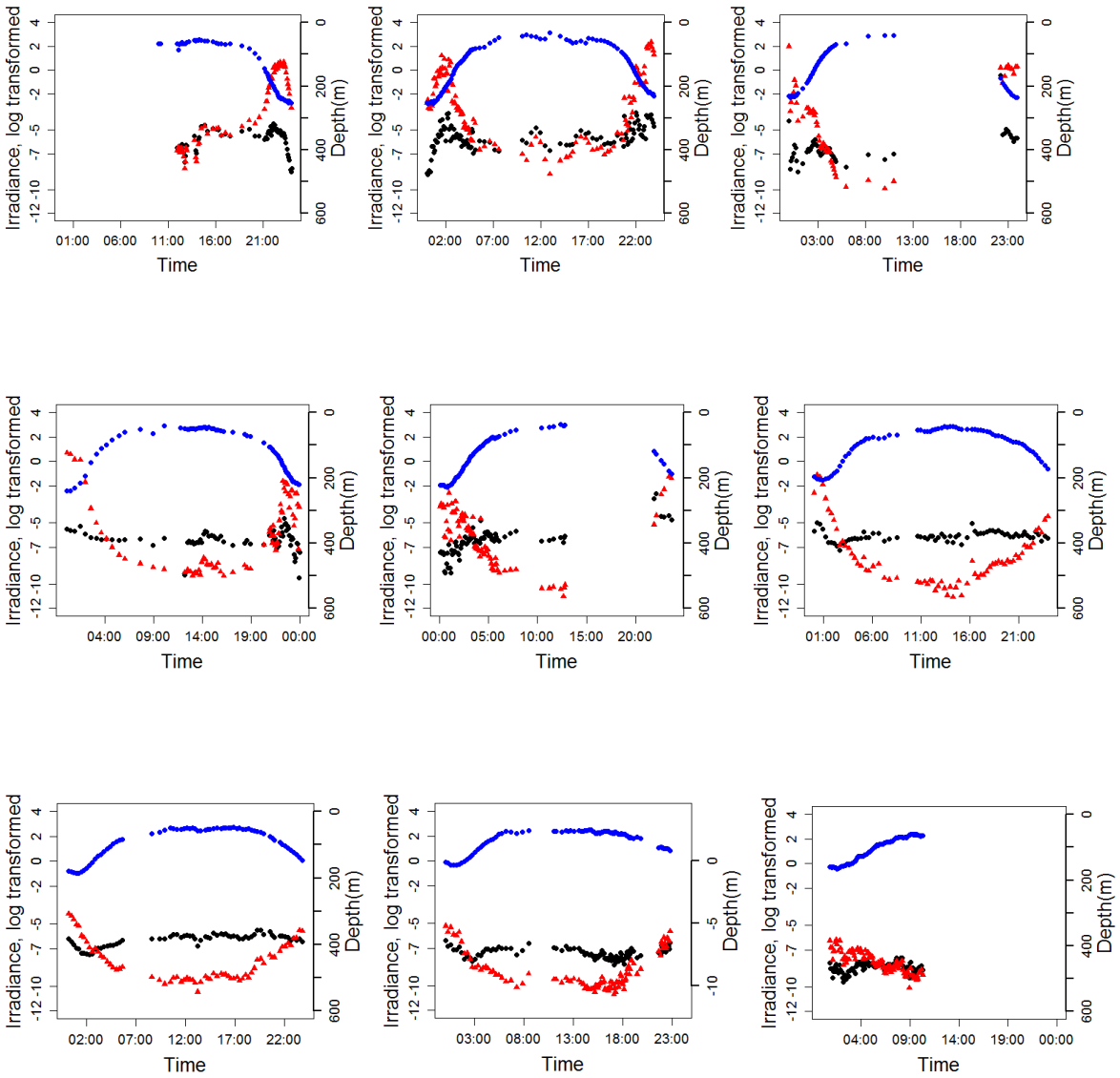

Figure 14. Diurnal distribution of log transformed surface irradiance (mW $m^{-2}nm^{-1}$ at 500 nm, blue), ambient irradiance levels at Z_m (mW $m^{-2}nm^{-1}$ at 500 nm, black) and Z_m (meters, red) for days, from upper left to lower right: 4th, 5th, 6th, 7th, 8th, 9th, 10th, 11th and 12th of May. The track begins in the eastern Norwegian Sea at 4th May and ends at the Icelandic Sea at 12th May.

3.5 Acoustics in relation to hydrographical data

I observed a decrease in mesopelagic biomass in parallel with a decrease in mean temperature and salinity (PSU) in the upper 600 m (Figure 15), and an increase in oxygen. Mean temperature decreases from 6 to 0 ˚C along the leg, while salinity (PSU) decreased from 35.1 to 34.9 PSU. Mean oxygen increased along the leg from 6.2 to 7.2 ml/l, but is close to saturation. Full saturation with temperature and salinity (PSU) composition similar to the

Norwegian Sea, corresponds to oxygen values between 8 and 10 ml/l (Green & Carritt, 1967).

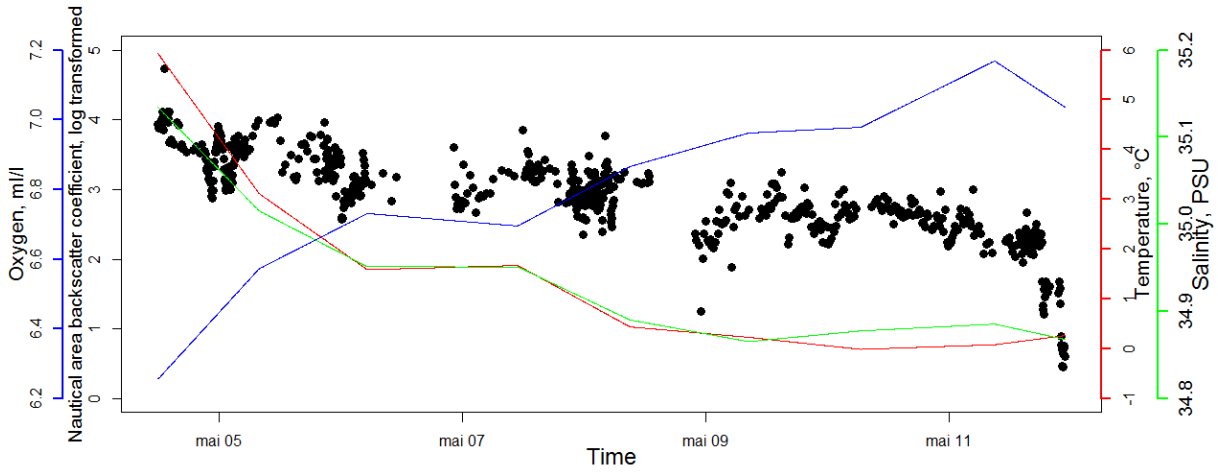

Figure 15. Mesopelagic s_A values, log transformed (black) and mean of temperature (˚C, red), Oxygen (ml/l, blue), and Salinity (PSU, green) during the leg for the upper 600 m. The track begins in the eastern Norwegian Sea at 4th May and ends at the Icelandic Sea at 12th May.

3.6 Biological catches from Harstad- and macrozooplankton trawl.

Benthosema glaciale dominated the mesopelagic fish caught in the trawl hauls, both the macrozooplankton trawl and the Harstad trawl. Mesopelagic fish specimens were caught at stations 102, 104, 105, 106, 110, 111 and 112. Details from the trawls are seen in Table 6. *B. glaciale* represented 82 % of mesopelagic fish caught by the Harstad trawl, and 68 % of mesopelagic fish caught by the Macrozooplankton trawl. *Notolepis* sp represented 18 % and 32 % respectively. *Maurolicus muelleri* was caught in the the Macrozooplankton trawl and represented less than 0.1 % and were considered negligible. The catches from the Harstad- and the macrozooplankton trawl in Table 7 are based on 4 hauls from the harstad trawl and 8 hauls from the Macrozooplankton trawl, and weighted in wet weight (g) (Table 6). 159 individuals of *B. glaciale* were sampled by 5 trawl hauls, 2 hauls from the Harstad trawl and 3 hauls from the Macrozooplankton trawl. All *B. glaciale* from the 5 trawl hauls was measured by length to nearest mm. 30 individuals from one trawl haul were weighted to nearest

decigram (Table 7, Figure 16). The mean length and weight from the all the catches was 52.6 mm and 2.3 g.

Table 6. Overview of biomass composition from the Macrozooplankton trawl and the Harstad trawl. Catches from the Macrozooplankton trawl comes from 8 hauls, while catches from the Harstad trawl comes from 4 hauls.

Group	Biomass (g wet weight) from Makrozooplankton trawl	Biomass (g wet weight) from Harstad trawl
Amphipoda	440.5	172
Epipelagic fish	0	280
Cephalopoda	1273	1341
Chaeotognatha	1198.25	40.5
Cnidaria	2878.95	340
Copepoda	123.5	57.5
Ctenophora	2063.3	778.5
Gastropoda	32	0
Euphausiacea	494.005	106.255
Mesopelagic fish	863.5	403.9
Nematoda	0	25.5
Shrimp	667.5	169.05

Table 7. Overview of *Benthosema glaciale* catches from the Macrozooplankton trawl and the Harstad trawls. Based on 5 hauls

Trawl station	Trawl type	Time of sampling	Latitude	Longitude	Depth (m)	Number of ind.	Mean length (mm)
102	Harstad trawl	19:26	65 15.82 N	0.54.43 W	310 - 290 m	20	57.9
104	Macrozooplankton trawl	00:50 – 01:58	65 39.70 N	2 53.58 W	1028 - 0 m	16	43.1
105	Macrozooplankton trawl	18:39 – 18:59	65 50.63 N	3 54.60 W	500 - 500 m	57	48.7
106	Macrozooplankton trawl	11:44 – 12:30	66 43.66 N	7 51.16 W	1000 - 0 m	36	55.9
112	Harstad trawl	12:42 – 13:12	68 12.73 N	15 31.50 W	510 - 490 m	30	57.7

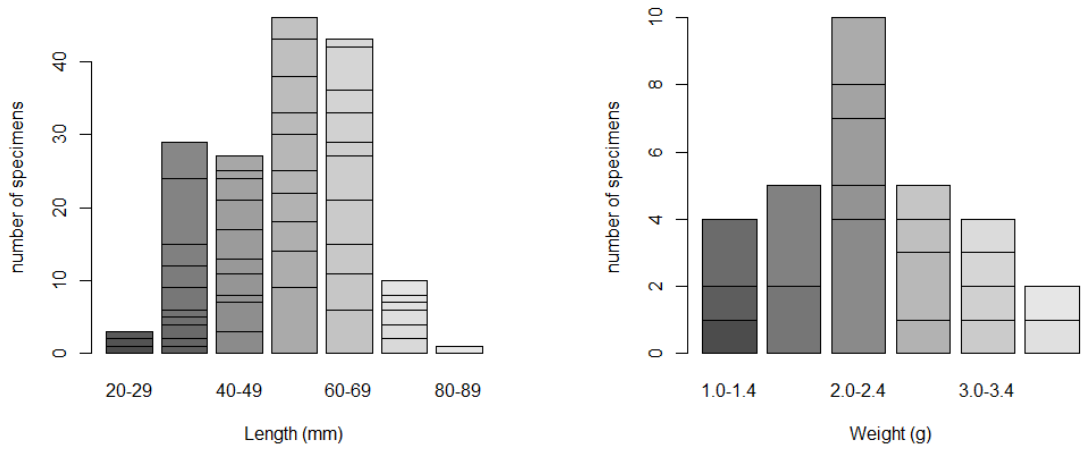

Figure 16. Length and weight distribution of *Benthosema glaciale*. Left: Length (mm) distribution of all trawl catches from stations 102, 104, 105, 106 and 112 (n = 159). Right: Weight (g) distribution of a subset, trawl station 112 (n = 30).

4.0 Discussion

The three main results in the present study are: (1) the depth variations of the MSL are consistent with DVM. (2) Night time distribution of the MSL became gradually deeper. (3) Lastly, the MSL biomass decreased along the track, as indicated by acoustics and subsequent conversion. The MSL was distributed deep during the day, shallow during the night and in between during dusk and dawn. This corresponds to a DVM pattern (Staby et al., 2011, Klevjer et al., 2012). The trawl catches showed the presence of the mesopelagic fish *Benthosema glaciale* that is known for conducting DVM (Dypvik et al., 2012a).

4.1 Factors governing the daily spatial patterns of the MSL

The study showed that the MSL have a spatio-temporal distribution that is interpreted as diel-vertical migration. There are several hypotheses attempting to explain what initiates diel-vertical migration. These hypotheses includes predator-avoidance (Eggers, 1978), foraging opportunities (Janssen and Brandt, 1980), bioenergetic (Brett, 1971), different hypotheses concerning light (Cohen and Forward, 2009) and oxygen minimum zones (OMZ) (Bianchi et al., 2013). My observations will be discussed accordingly with light regime, temperature gradients and oxygen minimum zones.

4.1.1 Light intensity as a governing factor for DVM

The role of light as a proximate for DVM was early studied in Daphnia (Ringelberg, 1964). Light has earlier been predicted to affect DVM behavior (Clark and Levy, 1988, Rosland and Giske, 1997, Han and Straskraba, 1998). Light regime was observed (Scheuerell and Schindler, 2003) to affect how diel vertical migrants hunt and avoid prey and predator, due to the importance of visual predation. There are four main hypothesis for light as a stimulus and predictor for DVM: (1) The isolume hypothesis, (2) aboslute intensity threshold hypothesis, (3) the rate-of-change hypothesis (Cohen and Forward, 2009), and (4) the antipredation window (Clark and Levy, 1988).

The results in the present study showed a correlation between surface irradiance and the MSL Z_m. This kind of relation has been observed in zooplankton (Frank and Widder, 1997) and mesopelagic fishes (Staby and Aksnes, 2011). My observations showed that the

distribution of the MSL Z_m were consistent with the surface irradiance patterns, in accordance with the characteristics of DVM.

My results showed that the ambient irradiance at the MSL Z_m had much less variation than the surface irradiance.

The isolume hypothesis, also known as the preferendum hypothesis, predicts that organisms follow a preferred, optimal light level, an isolume. DVM in *M. muelleri* was discussed in relation to a preferred isolume of light intensity by Balino and Aksnes (1993). *Meganyctiphanes norvegica* is observed conducting diel-vertical migration (Buchholz et al., 1995, Onsrud and Kaartvedt, 1998, Onsrud et al., 2004). The ambient light showed little variation in the upper spatial boundaries of the scattering layer that was comprised of *M. Norvegica* (Onsrud and Kaartvedt, 1998). The population seemed to follow an isolume across seasons, regardless of changes in temperature, oxygen and prey abundance. In Staby and Aksnes (2011), it was observed that the scattering layer ascribed for *M. muelleri*, was distributed within a preferred range of light intensity.

My observations did not show any consistency with the isolume hypothesis per se, since the ambient irradiance was not composed of a single light level. The observations showed that the ambient irradiance were within a large range of irradiance, which were several orders of magnitude.

The absolute intensity threshold hypothesis says that ascent and descent by an organism is initiated when the ambient light intensity changes below or above a specific threshold. Swift and Forward (1988) suggested that the absolute threshold might govern DVM in the freshwater insect larvae *Chaoborus punctipennis*. My observations found no evidence of a certain absolute threshold initiating DVM in the MSL Z_m, and the observations are therefore not consistent with this hypothesis.

The rate-of-change hypothesis states that the change in rate and direction of ambient light acts as cues for vertical movements. Instead of following an isolume, the organisms respond in situ to the relative rate of change in light. Several studies have attempted to determine the effect of this hypothesis (Ringelberg, 1964, Haney et al., 1990). According to Haney et al. (1990) the speed during ascent for *Chaoborus punctipennis* was proportional to the change

in light intensity. It were difficult to determine what effect rate-of-change might have in this study, since I do not have measurements in situ. Earlier studies rely mostly upon ponds and lakes were the populations and physical factors could be measured more effectively.

The antipredation window is another hypothesis attempting to explain the cues that initiate and govern DVM (Clark and Levy, 1988). The antipredation window is a more complete hypothesis than the three former since it is derived of evolutionary reasoning. It combines the effect of visual foraging opportunities and predation risk, as a function of the light regime. This means that the hypothesis combines both proximate and ultimate factors (Ringelberg and Van Gool, 2003), and centers around the trade-off between foraging and predator avoidance, and old and important element of ecology (Begon et al., 2006).

In the antipredation window hypothesis, vision and consequently light intensity and water clarity, is predicted to play a major role facilitating DVM behavior. The hypothesis predicts ambient light as proxy for the trade-off between predator avoidance and foraging opportunities, since the diel vertical migrant is both hunting and being hunted visually. The migrants are thereby predicted to distribute in accordance with the visual range, which again is a function of light. It is known that improved visual conditions can increase risk of predation from predators (Clark and Levy, 1988, Gregory and Northcote, 1993, Mazur and Beauchamp, 2003). Results from Mazur and Beauchamp (2003), showed that the migrants experienced highest predation risk by visual predators in waters with intermediate visual conditions. Poor visual conditions would thereby decrease success for both the migrants and predators to hunt, but if the visual condition improves too much, the prey would be forced to initiate DVM as an antipredation tactic (Zaret and Suffern, 1976, Clark and Levy, 1988).

Gliwicz (1986) observed that in lakes with longer presence of visual planktivorous predators, the copepods would display more distinct vertical distribution. It was observed that copepods did not perform DVM in lakes lacking predators. These results suggest that the presence of visual predators selects for DVM behavior. Scheuerell and Schindler (2003) observed that juvenile sockeye salmon distributed in accordance with a preferred light intensity range, and linked this to piscivorous predators. During observations in summertime, the variation of ambient light was greatly reduced compared to the variation of surface light. The autumn observation showed less discrepancy between the ambient and

surface light variations, but the variation of ambient light was still lower than the variation of surface irradiance.

My observations showed that the vertical distribution of the MSL Z_m was correlated to variation in surface irradiance. I also observed that the ambient irradiance at Z_m had less variation than the incident light. These observations are consistent with the antipredation window hypothesis, since the antipredation window hypothesis predicts that the migrants will occupy a specific range of visibility.

My observations suggest that the organisms of the MSL migrate and distribute in accordance with a preferred range of visibility, which is a function of the light regime. My observations suggest that this migration then caused the reduced variation in ambient irradiance. This would be consistent with the antipredation window hypothesis (Clark and Levy, 1988).

The variation in ambient irradiance was highest during dusk and dawn. There are several sources of error that affects underwater irradiance measurements. Wave actions, fluctuations of incident light by clouds, and solar elevation (Kirk, 1983). Waves can focus light to certain depths in the water column, causing increased variation of downwelling light. Short-term increase in cloud cover could facilitate greater variation in ambient light. It might not be enough time for the animals to migrate, instead causing short-term variation in ambient light. Solar elevation affects K, and thereby downwelling irradiance (Zheng et al., 2002). The solar elevation is low at dusk and dawn, and the attenuation coefficient thereby increases as the light beam must travel a longer distance in the water column.

Of these factors, solar elevation is likely causing most variation of ambient irradiance at dusk and dawn. Wave focusing and cloud cover would likely reinforce this variation even more. There might be unknown biological causes for the high variation in ambient light at dusk and dawn. My observations however, cannot explain any such biological causes for this increased variation.

There is also the possibility that the interpolated attenuation coefficient might suffer from errors. The extrapolated attenuation coefficients are questionable, since downwelling irradiance was only measured at 6 stations. If the in situ attenuation coefficients differed from the extrapolated values, the real ambient light levels would differ. The variation

throughout the time series however would likely not differ much, and the ambient light at Z_m would propably still vary much less than the surface irradiance.

4.1.2 Oxygen minimum zones as refuge for vertical migrants

It has been proposed that zones with low oxygen concentrations may act as refuge habitat against predators (Wishner et al., 1998). Bianchi et al. (2013) found that DVM daytime depths correlated with low oxygenated zones. They suggested that low oxygenated zones might serve as a refuge against predators. Their results included oxygen data on a global scale, with values varying between 40 – 200 mmol m^{-3} . These are levels well below the saturation points (Green and Carritt, 1967). Observations in habitat with low oxygen content, showed that several independent scattering layers had different daytime depths (Klevjer et al., 2012), some of the scattering layers occupied above the oxygen minimum zone (OMZ), others in the vicinity of the OMZ or below it. Mesopelagic fishes were also found at depths close to the hypoxic boundaries (Koslow et al., 2011), with oxygen content between 0.5 and 1.5 ml/l, which is quite extreme conditions which is close to hypoxia. It was speculated by Bianchi et al. (2013) that in absence of oxygen minimum zones, the vertical migrants may descend deeper to avoid predators. Due to the fact that my sampling area was nearly saturated with oxygen, there is no evidence that oxygen affected the spatio-temporal distribution of the MSL. I therefore rule oxygen out as a factor affecting vertical distribution of the MSL in the Norwegian Sea and Icelandic Sea.

4.1.3 The deeper night time distribution of the MSL along the track

The increased surface irradiance affected the DVM pattern of the MSL. My results showed that the MSL Z_m were distributed gradually deeper along the cruise track. The distribution of night time depths correlated with surface irradiance. The solar irradiance during night time increased with as much as 2 - 3 orders of magnitude along the track, while the attenuation coefficient decreased along the last part of the track. Water clarity affects the light regime through vertical extinction of light (Mobley, 1990, Kaiser et al. 2005). The observed decrease in attenuation coefficient will result in deeper penetration of light in the water column. My observations showed a correlation between the increased depths at night time and the

increased surface irradiance. These observations are consistent with the predictions of the antipredation window hypothesis

4.1.4 The diel-vertical migration of the MSL in relation to temperature

I cannot exclude the effect of temperature on either the DVM patterns or the increased depths of the MSL. The bioenergetic hypothesis states that temperature affects diel-vertical migration (Brett, 1971). The hypothesis predicts that metabolic costs and benefits initiate DVM in an animal by migrating through temperature gradients. Water masses or temperature trends might also force the MSL deeper along the track. I found no patterns between DVM and temperature gradients or water masses.

4.2 The decrease of biomass of the MSL in relation to water masses and light regime

The density and estimated biomass of the MSL decreased along the track. The mean s_A decreased from 5940 $m^2/\ n.mi^2$ at the 4th May to 185 $m^2/\ n.mi^2$ at the 11th May. The estimated biomass decreased from 260 $\frac{g}{m^2}$ to 4 $\frac{g}{m^2}$ during the same period.

There was a strong correlation between oxygen content in the mesopelagic zone and abundance of mesopelagic fishes in Koslow et al. (2011). Due to my results however, it is unlikely that oxygen affected the decrease in biomass along the track, due to the near oxygen saturation everywhere.

The decrease in biomass of the MSL was concurrent with a decrease in temperature along the cruise track. It was also observed that the biomass decreased westwards along a longitudinal gradient, by 24 longitudinal degrees. My observations showed hydrographical characteristics similar to previous studies in the Norwegian Sea (Skjoldal et al. 2004). Ocean currents are one of the major oceanographic factors affecting such composition and change (Pinet, P. 2009). Nordic Seas (Composed of the Norwegian Sea, Icelandic Sea and Greenland Sea) have two large currents, the Norwegian-Atlantic current (NAC) and the East Greenland current (EGC). The NAC contributes inflow of warm water from the south into the eastern Norwegian Sea, while the EGC brings colder water into the Icelandic Sea and western

Norwegian Sea from the arctic north (Skjoldal et al. 2004). The study area included Atlantic water (AW), Modified East Icelandic Water (MEIW), and Norwegian Sea Arctic Intermediate Water (NSDW).

The temperature change observed in this study seems to be in accordance with the change of inflowing AW, MEIW, NSDW (Skjoldal et al. 2004). Station 153 to 155 seems to be within the AW, with upper water temperature from 5 to 8 ˚C. From station 156 to 159 it seems to be in the MEIW, with temperatures between 4 to 2 ˚C. From station 160 to 165 it seems to be within NSDW, with temperatures between 1.5 to -0.5 ˚C. The first part of the track shows more distinct vertical gradients of temperature than the later parts, and seems consistent with AW.

There have been observed changes in mesopelagic community along temperature gradients (Collins et al., 2012). There was also speculated that the absence of *Benthosema glaciale* in the northern parts of the Labrador Sea might be due to colder water (Sameoto, 1989). O'Driscoll et al. (2011) observed that mesopelagic fish biomass in the southern Pacific Ocean and sub-Antarctic Ocean peaked at surface temperature of 15 – 16 ˚C. Figueroa et al. (1998) observed a change in mesopelagic fish community in accordance with water masses. The hydrographical data were sampled simultaneously, which could make it difficult to differentiate the effect of one physical factor from another, except from obviously oxygen.

In this study, the solar irradiance at night time increased by 2-3 orders of magnitude along the track, while the biomass decreased. Both the increased illumination and decrease in biomass were observed on a latitudinal gradient, as the cruise traveled north by 5 latitudinal degrees. Previous studies showed that zooplankton biomass at intermediate and higher latitudes decreased during summer (Brodeur and Ware, 1992). Decrease in biomass has been linked to latitude, both with zooplankton (Brodeur and Ware, 1992) and mesopelagic fish (O'Driscoll et al. 2011). Kaartvedt et al. (1998) speculated that presence of mesopealgic fishes in the Norwegian Sea decreases northwards due to more extreme light regimes like longer daylight during summer. There were also speculated that *B. glaciale* might be restricted by longer days and less dark hours (Sameoto, 1989). The area sampled in Sameoto (1989) are located on similar latitudes as my observations. It is also known that increased water clarity will result in better optical conditions for visual predation. Aksnes et al. (2004)

showed an inverse relationship between mesopelagic fish abundance and light absorbance in fjord systems.

The biomass decreased concurrently with a decrease in temperature and an increase in surface irradiance at night. As mentioned earlier it is difficult to determine which factor has the largest effect on biomass. This would require more than one survey. However, the attenuation coefficients did not differ greatly, and did not seem to show any patterns in accordance with Aksnes et al. (2004). Cold water and change in light regime could both facilitate an environment that might be less hospitable for the MSL occupants. My observations showed that the decrease in biomass was consistent with reduced temperature. My observations could not however, explain any potential effect of water clarity on the decrease in biomass.

4.3 The composition of the MSL

Benthosema glaciale was found on several stations, and is known to inhabit the Norwegian Sea (Torgersen et al., 1997, Dalpadado et al., 1998). The mesopelagic fishes in the biological sampling were dominated by *B. glaciale*, representing 68 % and 82 % of the weight (g) of the mesopelagic fish caught in the macrozooplankton trawl and the Harstad trawl respectively. Specimens of *Notolepis* sp. was also caught, representing 32 % (macrozooplankton trawl) and 18 % (Harstad trawl) of the weight (g) of all mesopelagic fish caught in the hauls. Jellyfish, krill, shrimp and copepods were also caught in the Harstad trawl and macrozooplankton trawl. The sampling capacity was severely reduced. The multisampler of the Harstad trawl did not function, which meant the samples could not be separated by depth. The number of hauls was also reduced due to time constraints and technical problems onboard. Past studies in the Norwegian Sea have indicated a dominance of *Benthosema glaciale* and *Maurolicus muelleri*. *Arctozenus risso* was also found, but in less abundance (Gjøsæter 1981, Toregersen et al 1997, Dalpadado et al. 1998).

Due to the reduced sampling capabilities, the composition of the MSL could not be established with confidence. It is reasonable that *B. glaciale* was a component of the MSL. *B. glaciale* was observed in the Norwegian Sea during this survey and in past surveys. However, it does not exclude the other mesopelagic fishes as components, and there might be other components in the MSL than mesopelagic fish. There are some jellyfish and zooplankton

which have been observed conducting DVM in the mesopelagic zone (Onsrud et al., 2004, Dupont et al., 2009). Mesopelagic fishes have been observed earlier to dominate the backscatter from 38 kHz (Kloser et al., 2009). There are also other animals that could have strong acoustic backscatter from 38 kHz. Many jellyfish have a much weaker backscatter at 38 kHz than mesopelagic fishes (Eiane et al., 1999). There are exceptions. Siphonophores and krill are known to inhabit scattering layers in the mesopelagic zone (Barham, 1966), and siphonephores has shown strong scattering strength from the lower frequencies 24 and 38 kHz (Warren, 2001, Trevorrow et al., 2005, Klevjer and Kaartvedt, 2006).

Siphonophores are known to occur in the Norwegian Sea (Bamstedt et al., 1998) and it was found in the present study in the western Norwegian/Icelandic Sea. Krill, copepods and shrimp were all present in the trawl catches. Likely candidates aside from mesopelagic fishes are gas-bearing jellyfish, zooplankton and larger crustaceans. The MSL is likely to have been composed by *B.glaciale*, yet other animals such as other jellyfish, zooplankton and larger crustaceans could possibly also be components.

4.4 The potential role of the MSL in the Norwegian Sea ecosystem

There are recent studies which suggests that biomass of mesopelagic fish are 1-2 order of magnitude higher (Irigoien et al., 2014) than previously estimated (Gjosaeter and Kawaguchi, 1980). Gjosaeter and Kawaguchi (1980) estimated a mean biomass of mesopelagic fishes in the Norwegian Sea between 0.5 – 2.0 $\frac{g}{m^2}$, based on trawl catches. If we in the present study assume that the MSL is composed of *B glaciale*, then a mean biomass of 67 $\frac{g}{m^2}$ ± 62 is indicated, which is between 1 – 2 orders of magnitude higher than the former estimates. This biomass estimate is based upon the assumption that the MSL constitutes *B. glaciale*. Species composition, target strength and weight values are critical assumptions to this estimate (Gjøsæter and Kawaguchi 1980, Irigoien et al 2014). Thus there are quite large uncertainties in the biomass estimates.

Diel vertical migration is considered an important element in export of different substances from surface waters (Hays et al., 2001), which can be carbon (Takahashi et al., 2009) and nitrogen (Steinberg et al., 2002). Steinberg et al. (2000) showed that migrant zooplankton

through active transport, were responsible for a large portion of carbon export. It has been suggested that diel-vertical migrants like mesopelagic fishes play a much larger role in the carbon flux than previously thought (Hernandez-Leon et al., 2010, Irigoien et al., 2014). Vertical migrants can affect the ecosystem by transporting carbon over hundred of meters (Irigoien et al., 2014). The migrants could consume food near surface during night and then within hours migrate to deeper water hundreds of meters below, were the animals die, defecate or are eaten. Without vertical migration, the organisms would be consumed in the shallow depths. With vertical migration the carbon would be transported directly to the deep water. The DVM could thereby contribute to ecosystem by transpassing a large part of the water column when transporting carbon or nitrogen.

To give an impression of what role the MSL might have in the Norwegian Sea, we have to make a few assumptions: (1) that the MSL distribution is DVM, (2) that it consists of mainly of *Benthosema glaciale* and (3) that earlier biomass estimates have been underestimated. Given these assumptions, the MSL appears to be quite important for the organic transport in the Norwegian Sea.

5.0 Conclusion

My observations suggested that *B. glaciale* is a major component of the MSL. My estimations showed that the MSL might be underestimated. This is however under certain assumptions and will suffer from several errors. The MSL distribution seemed to be governed by light regime. The mean depth of the MSL (Z_m) appeared to be within a certain range of ambient irradiance. Due to migration this ambient irradiance showed far less variation than the surface irradiance along the track. Other physical factors did not seem to correlate with the DVM pattern. These results suggest that DVM of the mesopelagic scattering layer emerges from a tendency for the organisms of the layer to stay in a certain light regime. Based on predictions from the antipredation window hypothesis, one might speculate that the observed DVM is an adaption of the MSL organisms that emerges from the trade-off between predation risk and foraging opportunities.

Acknowledgements:

From the bottom of the ocean I thank my two supervisors during the work of this thesis, Professor Dag Lorents Aksnes, UIB and TEG, and Dr. Thor Aleksander Klevjer, IMR, for great help, guidance and fast response and valuable constructive critique of my work. I wish to thank my parents, brothers, friends and family for moral support and enjoyable discussions. I also wish to thank Dr. Daniel Ricard, Dr. Anders Frugård Opdal, Dr. Rune Rosland and M.Sc. Bjørn Snorre Anderssen for statistical help. I also wish to thank M.Sc. Sindre Fonkalsrud and M.Sc Kristian Thinn Solheim for comments on elements in the thesis, even though 'below sea level' is not necessary to include when denoting 'depth (m)'. I wish to thank the Theoretical Ecology Group (TEG) for great feedback and enjoyable lunch. I also wish to thank the crew of the G.O Sars and the science team onboard for good company during the survey. Lastly, I wish to thank the University in Bergen (UiB), the Institute of Marine Research (IMR) and the EURO-BASIN program for the survey.

6.0 References

AKSNES, D. L., NEJSTGAARD, J., SOEDBERG, E. & SØRNES, T. 2004. Optical control of fish and zooplankton populations. *Limnology and Oceanography,* 49**,** 233-238.

BAGØIEN, E., KAARTVEDT, S., AKSNES, D. L. & EIANE, K. 2001. Vertical distribution and mortality of overwintering Calanus. *Limnology and Oceanography,* 46**,** 1494-1510.

BALINO, B. M. & AKSNES, D. L. 1993. Winter distribution and migration of the sound-scattering layers, zooplankton and micronekton in masfjorden, western norway. *Marine Ecology Progress Series,* 102**,** 35-50.

BÅMSTEDT, U., FOSSA, J. H., MARTINUSSEN, M. B. & FOSSHAGEN, A. 1998. Mass occurrence of the physonect siphonophore *Apolemia uvaria* (LESUEUR) in Norwegian waters. *Sarsia,* 83**,** 79-85.

BARHAM, E. G. 1966. Deep scattering layer migration and composition - observations from a diving saucer. *Science,* 151**,** 1399-&.

BARRETT, R. 2002. Food consumption by seabirds in Norwegian waters. *ICES Journal of Marine Science,* 59**,** 43-57.

BEGON, M., TOWNSEND, C. R. & HARPER, J. L. 2006. Ecology: from individuals to ecosystems. 4th edition. Blackwell Publishing

BIANCHI, D., GALBRAITH, E. D., CAROZZA, D. A., MISLAN, K. A. S. & STOCK, C. A. 2013. Intensification of open-ocean oxygen depletion by vertically migrating animals. *Nature Geoscience,* 6**,** 545-548.

BRETT, J. R. 1971. Energetic responses of salmon to temperature - study of some thermal relations in physiology and freshwater ecology of sockeye salmon (*Oncorhynchus nerka*). *American Zoologist,* 11**,** 99-&.

BRODEUR, R. D. & WARE, D. M. 1992. Long-term viability in zooplankton biomass in the subarctic Pacific Ocean. *Fisheries Oceanography,* 1.

BUCHHOLZ, F., BUCHHOLZ, C., REPPIN, J. & FISCHER, J. 1995. Diel vertical migrations of *Meganyctiphanes norvegica* in the kattegat - comparison of net catches and measurements with acoustic doppler current profilers. *Helgolander Meeresuntersuchungen,* 49**,** 849-866.

CATUL, V., GAUNS, M. & KARUPPASAMY, P. K. 2011. A review on mesopelagic fishes belonging to family Myctophidae. *Reviews in Fish Biology and Fisheries,* 21**,** 339-354.

CLARK, C. W. & LEVY, D. A. 1988. Diel vertical migrations by juvenile sockeye salmon and the antipredation window. *American Naturalist,* 131**,** 271-290.

COHEN, J. H. & FORWARD, R. B., JR. 2009. Zooplankton diel vertical migration - a review of proximate control. *Oceanography and Marine Biology: An Annual Review, Vol 47.*

COLLINS, M. A., STOWASSER, G., FIELDING, S., SHREEVE, R., XAVIER, J. C., VENABLES, H. J., ENDERLEIN, P., CHEREL, Y. & VAN DE PUTTE, A. 2012. Latitudinal and bathymetric patterns in the distribution and abundance of mesopelagic fish in the Scotia Sea. *Deep Sea Research Part II: Topical Studies in Oceanography,* 59-60**,** 189-198.

DALE, T., BAGØIEN, E., MELLE, W. & KAARTVEDT, S. 1999. Can predator avoidance explain varying overwintering depth of Calanus in different oceanic water masses? *Marine Ecology Progress Series,* 179**,** 113-121.

DALPADADO, P., ELLERTSEN, B., MELLE, W. & SKJOLDAL, H. R. 1998. Summer distribution patterns and biomass estimates of macrozooplankton and micronekton in the Nordic Seas. *Sarsia,* 83**,** 103-116.

DEL GIORGIO, P. A. & DUARTE, C. M. 2002. Respiration in the open ocean. *Nature,* 420**,** 379-384.

DUPONT, N. & AKSNES, D. L. 2012. Effects of bottom depth and water clarity on the vertical distribution of Calanus spp. *Journal of Plankton Research,* 34**,** 263-266.

DUPONT, N., KLEVJER, T. A., KAARTVEDT, S. & AKSNES, D. L. 2009. Diel vertical migration of the deep-water jellyfish *Periphylla periphylla* simulated as individual responses to absolute light intensity. *Limnology and Oceanography,* 54**,** 1765-1775.

DYPVIK, E., KLEVJER, T. A. & KAARTVEDT, S. 2012a. Inverse vertical migration and feeding in glacier lanternfish (*Benthosema glaciale*). *Mar Biol,* 159**,** 443-453.

DYPVIK, E., RØSTAD, A. & KAARTVEDT, S. 2012b. Seasonal variations in vertical migration of glacier lanternfish. *Mar Biol,* 159**,** 1673-1683.

EGGERS, D. M. 1978. Limnetic feeding-behavior of juvenile sockeye salmon in lake washington and predator avoidance. *Limnology and Oceanography,* 23**,** 1114-1125.

EIANE, K., AKSNES, D. L., BAGOIEN, E. & KAARTVEDT, S. 1999. Fish or jellies - a question of visibility? *Limnology and Oceanography,* 44**,** 1352-1357.

EIANE, K., AKSNES, D. L., OHMAN, M. D., WOOD, S. & MARTINUSSEN, M. B. 2002. Stage-specific mortality of Calanus spp. Under different predation regimes. *Limnology and Oceanography,* 47**,** 636-645.

FIGUEROA, D. E., DE ASTARLOA, J. M. D. & MARTOS, P. 1998. Mesopelagic fish distribution in the southwest Atlantic in relation to water masses. *Deep-Sea Research Part I-Oceanographic Research Papers,* 45**,** 317-332.

FRANK, T. M. & WIDDER, E. A. 1997. The correlation of downwelling irradiance and staggered vertical migration patterns of zooplankton in Wilkinson Basin, Gulf of Maine. *Journal of Plankton Research,* 19**,** 1975-1991.

GJØSÆTER, J. 1981. Growth, production and reproduction of the myctophid fish *Benthosema glaciale* from western Norway and the adjacent seas. *Fiskeridirektoratets Skrifter Serie Havundersokelser,* 17**,** 79-108.

GJØSÆTER, J. & KAWAGUCHI, K. 1980. A review of the world resources of mesopelagic fish. *FAO Fisheries Technical Paper*.

GLIWICZ, M. Z. 1986. Predation and the evolution of vertical migration in zooplankton. *Nature,* 320**,** 746-748.

GREEN, E. J. & CARRITT, D. E. 1967. New tables for oxygen saturation of seawater. *Journal of Marine Research,* 25**,** 140-&.

GREGORY, R. S. & NORTHCOTE, T. G. 1993. Surface, planktonic, and benthic foraging by juvenile chinook salmon (*Oncorhynchus tshawytscha*) in turbid laboratory conditions. *Canadian Journal of Fisheries and Aquatic Sciences,* 50**,** 233-240.

HAN, B. P. & STRASKRABA, M. 1998. Modeling patterns of zooplankton diel vertical migration. *Journal of Plankton Research,* 20**,** 1463-1487.

HANEY, J. F., CRAGGY, A., KIMBALL, K. & WEEKS, F. 1990. Light control of evening vertical migrations by *chaoborus punctipennis* larvae. *Limnology and Oceanography,* 35**,** 1068-1078.

HAYS, G. C. 2003. A review of the adaptive significance and ecosystem consequences of zooplankton diel vertical migrations. *Hydrobiologia,* 503**,** 163-170.

HAYS, G. C., HARRIS, R. P. & HEAD, R. N. 2001. Diel changes in the near-surface biomass of zooplankton and the carbon content of vertical migrants. *Deep-Sea Research Part Ii-Topical Studies in Oceanography,* 48**,** 1063-1068.

HERNANDEZ-LEON, S., FRANCHY, G., MOYANO, M., MENENDEZ, I., SCHMOKER, C. & PUTZEYS, S. 2010. Carbon sequestration and zooplankton lunar cycles: Could we be missing a major component of the biological pump? *Limnology and Oceanography,* 55**,** 2503-2512.

HOPKINS, T. L., SUTTON, T. T. & LANCRAFT, T. M. 1996. The trophic structure and predation impact of a low latitude midwater fish assemblage. *Progress in Oceanography,* 38**,** 205-239.

IRIGOIEN, X., KLEVJER, T. A., RØSTAD, A., MARTINEZ, U., BOYRA, G., ACUNA, J. L., BODE, A., ECHEVARRIA, F., GONZALEZ-GORDILLO, J. I., HERNANDEZ-LEON, S., AGUSTI, S., AKSNES, D. L., DUARTE, C. M. & KAARTVEDT, S. 2014. Large mesopelagic fishes biomass and trophic efficiency in the open ocean. *Nat Commun,* 5**,** 3271.

ISAACS, J. D., TONT, S. A. & WICK, G. L. 1974. Deep scattering layers - vertical migration as a tactic for finding food. *Deep-Sea Research,* 21**,** 651-656.

JANSSEN, J. & BRANDT, S. B. 1980. Feeding ecology and vertical migration of adult alewives (*Alosa pseudoharengus*) in lake-michigan. *Canadian Journal of Fisheries and Aquatic Sciences,* 37**,** 177-184.

KAARTVEDT, S. 2000. Life history of *Calanus finmarchicus* in the Norwegian Sea in relation to planktivorous fish. *ICES Journal of Marine Science,* 57**,** 1819-1824.

KAARTVEDT, S., KNUTSEN, T. & HOLST, J. C. 1998. Schooling of the vertically migrating mesopelagic fish *Maurolicus muelleri* in light summer nights. *Marine Ecology Progress Series,* 170**,** 287-290.

KAARTVEDT, S., RØSTAD, A., KLEVJER, T. A. & STABY, A. 2009. Use of bottom-mounted echo sounders in exploring behavior of mesopelagic fishes. *Marine Ecology Progress Series,* 395**,** 109-118.

KAARTVEDT, S., STABY, A. & AKSNES, D. L. 2012. Efficient trawl avoidance by mesopelagic fishes causes large underestimation of their biomass. *Marine Ecology Progress Series,* 456**,** 1-6.

KAARTVEDT, S., TORGERSEN, T., KLEVJER, T. A., RØSTAD, A. & DEVINE, J. A. 2008. Behavior of individual mesopelagic fish in acoustic scattering layers of Norwegian fjords. *Marine Ecology Progress Series,* 360**,** 201-209.

KAISER, M. J., ATTRILL, M. J., JENNINGS, S., THOMAS, D. N., BARNES, D. K. A., BRIERLEY, A. S., POLUNIN, N. V. C., RAFFAELLI, D. G. & WILLIAMS, P. J. L. B. 2005. Marine ecology: processes, systems and impacts.

KIRK, J. T. O. 1983. Light and photosynthesis in aquatic ecosystems. Cambridge University Press, Cambridge, London etc.

KLEVJER, T. & KAARTVEDT, S. 2006. In situ target strength and behaviour of northern krill (*Meganyctiphanes norvegica*). *ICES Journal of Marine Science,* 63**,** 1726-1735.

KLEVJER, T. A., TORRES, D. J. & KAARTVEDT, S. 2012. Distribution and diel vertical movements of mesopelagic scattering layers in the Red Sea. *Mar Biol,* 159**,** 1833-1841.

KLOSER, R. J., RYAN, T. E., YOUNG, J. W. & LEWIS, M. E. 2009. Acoustic observations of micronekton fish on the scale of an ocean basin: potential and challenges. *Ices Journal of Marine Science,* 66**,** 998-1006.

KOSLOW, J. A., GOERICKE, R., LARA-LOPEZ, A. & WATSON, W. 2011. Impact of declining intermediate-water oxygen on deepwater fishes in the California Current. *Marine Ecology Progress Series,* 436**,** 207-218.

LARA-LOPEZ, A. L., DAVISON, P. & KOSLOW, J. A. 2012. Abundance and community composition of micronekton across a front off Southern California. *Journal of Plankton Research,* 34**,** 828-848.

MARCHAL, E. & LEBOURGES, A. 1996. Acoustic evidence for unusual diel behaviour of a mesopelagic fish (*Vinciguerria nimbaria*) exploited by tuna. *Ices Journal of Marine Science,* 53**,** 443-447.

MAZUR, M. M. & BEAUCHAMP, D. A. 2003. A comparison of visual prey detection among species of piscivorous salmonids: effects of light and low turbidities. *Environmental Biology of Fishes,* 67**,** 397-405.

MCCLATCHIE, S. & DUNFORD, A. 2003. Estimated biomass of vertically migrating mesopelagic fish off New Zealand. *Deep-Sea Research Part I-Oceanographic Research Papers,* 50**,** 1263-1281.

MOBLEY, C., D. 1994. Light and Water: Radiative Transfer in Natural Waters. Academic Press, Inc.

ONSRUD, M. S. R. & KAARTVEDT, S. 1998. Diel vertical migration of the krill *Meganyctiphanes norvegica* in relation to physical environment, food and predators. *Marine Ecology Progress Series,* 171**,** 209-219.

ONSRUD, M. S. R., KAARTVEDT, S., RØSTAD, A. & KLEVJER, T. A. 2004. Vertical distribution and feeding patterns in fish foraging on the krill *Meganyctiphanes norvegica*. *Ices Journal of Marine Science,* 61**,** 1278-1290.

O'DRISCOLL, R., L., HURST, R., J., DUNN, M., R., GAUTHIER, S., BALLARA, S., L. 2011. Trends in relative mesopelagic biomass using time series of acoustic backscatter data from trawl surveys. *New Zealand Aquatic Environment and Biodiversity Report No. 76*.

PALOMERA, I., OLIVAR, M. P., SALAT, J., SABATES, A., COLL, M., GARCIA, A. & MORALES-NIN, B. 2007. Small pelagic fish in the NW Mediterranean Sea: An ecological review. *Progress in Oceanography,* 74**,** 377-396.

PAULY, D., TRITES, A. W., CAPULI, E. & CHRISTENSEN, V. 1998. Diet composition and trophic levels of marine mammals. *Ices Journal of Marine Science,* 55**,** 467-481.

PEPIN, P. 2013. Distribution and feeding of Benthosema glaciale in the western Labrador Sea: Fish–zooplankton interaction and the consequence to calanoid copepod populations. *Deep Sea Research Part I: Oceanographic Research Papers,* 75**,** 119-134.

PINET, P., R. 2009. Invitation to Oceanography, Fifth edition. *Jones and Bartlett Publishers Canada.*

RINGELBERG, J. 1964. The positive phototatic reaction of *Daphnia magna Straus* : a contribution to the understanding of diurnal vertical migration. *Netherlands Journal of Sea Research,* 2.

RINGELBERG, J. & VAN GOOL, E. 2003. On the combined analysis of proximate and ultimate aspects in diel vertical migration (DVM) research. *Hydrobiologia,* 491**,** 85-90.

ROSLAND, R. & GISKE, J. 1997. A dynamic model for the life history of *Maurolicus muelleri*, a pelagic planktivorous fish. *Fisheries Oceanography,* 6**,** 19-34.

SAMEOTO, D. 1989. Feeding ecology of the lantern fish *Benthosema glaciale* in a subarctic region. *Polar Biology,* 9**,** 169-178.

SCHEUERELL, M. D. & SCHINDLER, D. E. 2003. Diel vertical migration by juvenile sockeye salmon: Empirical evidence for the antipredation window. *Ecology,* 84**,** 1713-1720.

SHEA, E. K. & VECCHIONE, M. 2010. Ontogenic changes in diel vertical migration patterns compared with known allometric changes in three mesopelagic squid species suggest an expanded definition of a paralarva. *Ices Journal of Marine Science,* 67**,** 1436-1443.

SIMMOND, J., MACLENNAN, D., N. 2005. Fisheries Acoustics: Theory and Practice, 2nd Edition. Blackwell Publishing.

SIOKOU, I., ZERVOUDAKI, S. & CHRISTOU, E. D. 2013. Mesozooplankton community distribution down to 1000 m along a gradient of oligotrophy in the Eastern Mediterranean Sea (Aegean Sea). *Journal of Plankton Research,* 35**,** 1313-1330.

SKJOLDAL, H., R. 2004. The Norwegian Sea ecosystem. Tapir Academic Press.

STABY, A. & AKSNES, D. L. 2011. Follow the light—diurnal and seasonal variations in vertical distribution of the mesopelagic fish *Maurolicus muelleri Marine Ecology Progress Series,* 422**,** 265-273.

STABY, A., RØSTAD, A. & KAARTVEDT, S. 2011. Long-term acoustical observations of the mesopelagic fish *Maurolicus muelleri* reveal novel and varied vertical migration patterns. *Marine Ecology Progress Series,* 441**,** 241-255.

STABY, A., SRISOMWONG, J., ROSLAND, R. 2013. Variation in DVM behaviour of juvenile and adult pearlside (*Maurolicus muelleri*) linked to feeding strategies and related predation risk. *Fisheries Oceanography*, 22, 90-101.

STEINBERG, D. K., CARLSON, C. A., BATES, N. R., GOLDTHWAIT, S. A., MADIN, L. P. & MICHAELS, A. F. 2000. Zooplankton vertical migration and the active transport of dissolved organic and inorganic carbon in the Sargasso Sea. *Deep-Sea Research Part I-Oceanographic Research Papers,* 47**,** 137-158.

STEINBERG, D. K., GOLDTHWAIT, S. A. & HANSELL, D. A. 2002. Zooplankton vertical migration and the active transport of dissolved organic and inorganic nitrogen in the Sargasso Sea. *Deep-Sea Research Part I-Oceanographic Research Papers,* 49**,** 1445-1461.

SUTTON, T. T., PORTEIRO, F. M., HEINO, M., BYRKJEDAL, I., LANGHELLE, G., ANDERSON, C. I. H., HORNE, J., SØILAND, H., FALKENHAUG, T., GODØ, O. R. & BERGSTAD, O. A. 2008. Vertical structure, biomass and topographic association of deep-pelagic fishes in relation to a mid-ocean ridge system. *Deep Sea Research Part II: Topical Studies in Oceanography,* 55**,** 161-184.

SWIFT, M. C. & FORWARD, R. B. 1988. Absolute light-intensity vs rate of relative change in light-intensity - the role of light in the vertical migration of *Chaoborus punctipennis* larvae. *Bulletin of Marine Science,* 43**,** 604-619.

TAKAHASHI, K., KUWATA, A., SUGISAKI, H., UCHIKAWA, K. & SAITO, H. 2009. Downward carbon transport by diel vertical migration of the copepods *Metridia pacifica* and *Metridia okhotensis* in the Oyashio region of the western subarctic Pacific Ocean. *Deep Sea Research Part I: Oceanographic Research Papers,* 56**,** 1777-1791.

TORGERSEN, T., KAARTVEDT, S., MELLE, W. & KNUTSEN, T. 1997. Large scale distribution of acoustical scattering layers at the Norwegian continental shelf and the eastern Norwegian Sea. *Sarsia,* 82**,** 87-96.

TREVORROW, M. V., MACKAS, D. L. & BENFIELD, M. C. 2005. Comparison of multifrequency acoustic and in situ measurements of zooplankton abundances in Knight Inlet, British Columbia. *The Journal of the Acoustical Society of America,* 117**,** 3574.

WARREN, J. 2001. In situ measurements of acoustic target strengths of gas-bearing siphonophores. *ICES Journal of Marine Science,* 58**,** 740-749.

WILSON, R. W., MILLERO, F. J., TAYLOR, J. R., WALSH, P. J., CHRISTENSEN, V., JENNINGS, S. & GROSELL, M. 2009. Contribution of Fish to the Marine Inorganic Carbon Cycle. *Science,* 323**,** 359-362.

WISHNER, K. F., GOWING, M. M. & GELFMAN, C. 1998. Mesozooplankton biomass in the upper 1000 m in the Arabian Sea: overall seasonal and geographic patterns, and relationship to oxygen gradients. *Deep-Sea Research Part Ii-Topical Studies in Oceanography,* 45**,** 2405-2432.

ZARET, T. M. & SUFFERN, J. S. 1976. Vertical migration in zooplankton as a predator avoidance mechanism. *Limnology and Oceanography,* 21**,** 804-813.

ZHENG, X. B., DICKEY, T. & CHANG, G. 2002. Variability of the downwelling diffuse attenuation coefficient with consideration of inelastic scattering. *Applied Optics,* 41**,** 6477-6488.

Appendix

1. Estimation of attenuation coefficient

It was decided to use the irradiance measurements obtained during lowering. There were several reasons for this. First, the horizontal drift of the instrument away from the ship was smallest during lowering, which ensured the least possible deviation from a vertical movement, and thereby minimizing deviations from an ideal upward facing light sensor. Secondly it seemed reasonable to minimizing the time used to measure the underwater irradiance by not using measurements from both lowering and when pulling up. For some stations attenuation coefficients were calculated for separate parts of the water column. The rationales for these choices are given, for each of the stations, in the next.

Station 153

The observations of the logarithm of the downwelling irradiances (Figure 1A) fits a straight line with a R^2 = 0.998 and K_d of 0.0495 m^{-1} is indicated. The data points in red indicate PAR measurements within the time of underwater measuring with the spectroradiometer (Figure 1B). We see a change of atmospheric PAR during the period of measuring, around 45 % increase. This correspond to a a relatively small error in the calculated attenuation by 8 %, from 0.050 to 0.054 M^{-1} (See eq. 10). Thus, changing incoming atmospheric light during the registrations might have introduced some uncertainty in the estimated attenuation coefficient at this station. The vertical profile of σ_t (Figure 1C) shows small σ_t variation down to around 100 m (the deepest irradiance measurement). The fluorescence, however, dropped between 70 and 100 m to less than 0.2 mg chl m^{-3}.

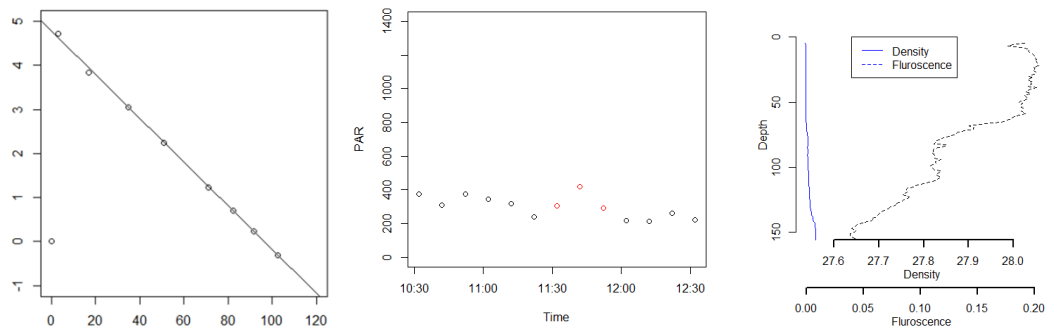

Figure 1. Left: Linear regression of downwelling irradiance at Station 153, downwards. X-axis represent depth, y-axis represent downwelling irradiance. -0.0495X + 4.7738, R^2= 0.9989, SD error : 0.0006, Right: Time series of PAR measurements before, during and after station 153. Red indicates PAR values during downwelling irradiance measurements. Under: σ_t and Fluorescence (mg chl m^{-3}) along depth (m), station 153.

Station 155:

The observations of the logarithm of the downwelling irradiance (Figure 2A) fits a straight line with a R^2 = 0.997 and K_d of 0.0498 m^{-1} is indicated. The data points in red indicate change in atmospheric PAR measurements during the underwater measurements with the spectroradiometer (Figure 2B). We see a relatively small change in attenuation by 0.4 %, from 0.0499 to 0.0501 M^{-1} (See eq. 10), which seems reasonable with the time of the day. The vertical profile of σ_t (Figure 2C) shows a larger variation than station 153, yet small one. The fluorescence showed fluctuating changes for much of the depth, but at relatively small levels (chlorophyll < 0.2 mg chl m^{-3})

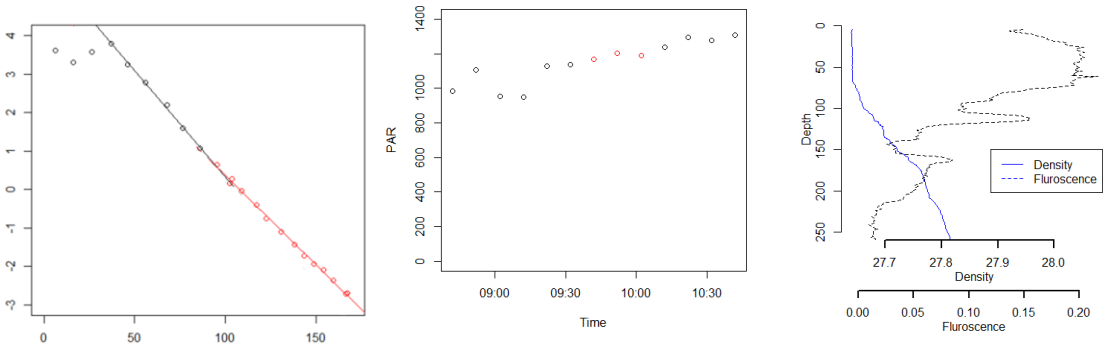

Figure 2. Left: Linear regression of downwelling irradiance, at Station 155, downwards. X-axis represent depth, y-axis represent downwelling irradiance. -0.0498X + 5.4851, R^2= 0.997, SD error : 0.0006. Right: Time series of PAR measurements before, during and after station 155. Red indicates PAR values during downwelling irradiance measurements. Under: σ_t and Fluorescence (mg chl m^{-3}) along depth (m), at station 155.

Station 158:

The observations of the logarithm of the downwelling irradiance (Figure 3A) are isolated in to straight lines over and under 90 meters, with R^2 = 0.998 and K_d of 0.0674 m^{-1} and R^2 = 0.998 and K_d of 0.0387 m^{-1}. The data points in red indicate atmospheric PAR measurements within the time of underwater measuring with the spectroradiometer (Figure 3B). We see a large decrease, by nearly 47 %, when lowering. This corresponds to a relatively small change in attenuation by 3.8 %, from 0.052 to 0.054 M^{-1} (See eq. 10). We see a change in the vertical profile of σ_t (Figure 3C) around 90 meters, which is considerable. Fluorescence shows a large decrease in the same depth, at slightly larger levels than the other stations (chlorophyll < 0.4 mg chl m^{-3}). It was therefore decided to split into two linear regressions of downwelling irradiance.

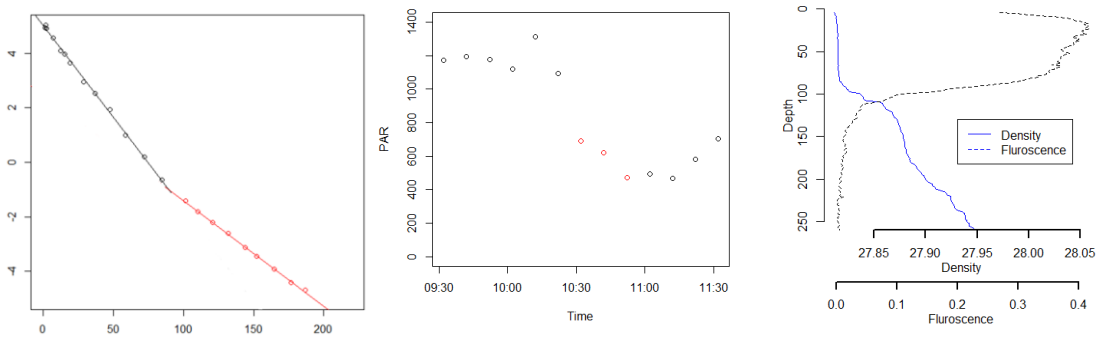

Figure 3. Left: Linear regression of downwelling irradiance at Station 158, downwards. X-axis represent depth, y-axis represent downwelling irradiance. -0.0674X + 5.0212, R2: 0.998, SD error: 0.0008, -0.0387X + 2.4617, R2: 0.9985, SD error: 0.0005. Right: Time series of PAR measurements before, during and after station 158. Red indicates PAR values during downwelling irradiance measurements. Under: σ_t and fluorescence (mg chl m^{-3}) along depth (m), at station 158.

Station 160:

The observations of the logarithm of the downwelling irradiance (Figure 4A) are isolated in to straight lines over and under 110 meters, with R^2 = 0.995 and K_d of 0.0541 m^{-1} and R^2 = 0.998 and K_d of 0.0357 m^{-1}. The data points in red indicate atmospheric PAR measurements within the time of underwater measuring with the spectroradiometer (Figure 4B). It shows

changes in during lowering, around 36 % decrease in PAR. This corresponds to a relatively small change in attenuation by 2.2 %, from 0.045 to 0.046 M^{-1} (See eq. 10). The vertical profile of σ_t (Figure 4C) shows a large change around 110 meters, while fluorescence have a large change around 40-60 meters, and later at the same depth as σ_t (chlorophyll < 0.2 mg chl m^{-3}).. It was therefore decided to split into two linear regressions of downwelling irradiance.

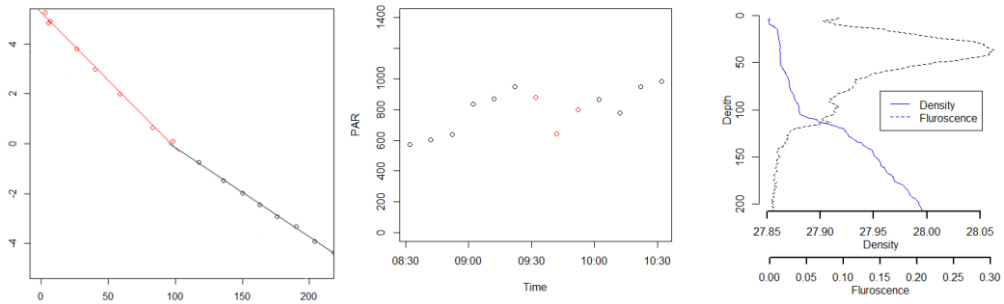

Figure 4. Left: Linear regression of downwelling irradiance at Station 160, downwards. X-axis represent depth, y-axis represent downwelling irradiance. -0.0541X + 5.2419, R2: 0.9957, Sd error: 0.0013

-0.0357X + 3.4101, R2: 0.9987, Sd error: 0.0004. Middle: Time series of PAR measurements before, during and after station 160. Red indicates PAR values during downwelling irradiance measurements. Right: σ_t and fluorescence (mg chl m^{-3}) along depth (m), at station 160.

Station 161:

The observations of the logarithm of the downwelling irradiance (Figure 5A) are isolated in to straight lines over and under 135 meters, with R^2 = 0.998 and K_d of 0.0427 m^{-1} and R^2 = 0.997 and K_d of 0.0367 m^{-1}. The data points in red indicate atmospheric PAR measurements within the time of underwater measuring with the spectroradiometer (Figure 5B). It indicates little change, around 2.5 %, and a small and steady increase of atmospheric PAR. This corresponds to a relatively small change in attenuation by 0.25 %, from 0.0396 to 0.0397 M^{-1} (See eq. 10). While the vertical profile of σ_t (Figure 5C) shows a large change around 135 meters. Fluorescence shows changes at the same depth, and much higher up, at around 30-40 meters (chlorophyll < 0.2 mg chl m^{-3}). It was therefore decided to split into two linear regressions of downwelling irradiance.

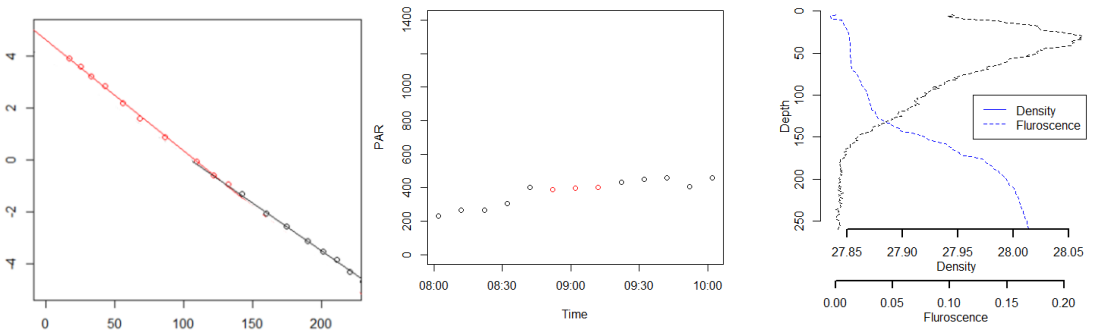

Figure 5. Left: Linear regression of downwelling irradiance at Station 161, downwards. X-axis represent depth, y-axis represent downwelling irradiance. - 0.0427334X + 4.6128096, R^2 = 0.9986, SD error: 0.0005411. -0.0367344X + 3.8504714, R^2 0.9972, SD error: 0.0006859. Middle: Time series of PAR measurements before, during and after station 161. Red indicates PAR values during downwelling irradiance measurements. Right: σ_t and fluroscence (mg chl m^{-3})along depth (m), at station 161.

Station 162:

The observations of the logarithm of the downwelling irradiance (Figure 6A) are isolated in to straight lines over and under 100 meters, with R^2 = 0.998 and K_d of 0.0470 m^{-1} and R^2 = 0.996 and K_d of 0.0369 m^{-1}. The data points in red indicate atmospheric PAR measurements within the time of underwater measuring with the spectroradiometer (Figure 6B). It shows a large, but steady change of atmospheric PAR during the period of measuring, around 54 %. This corresponds to a relatively small change in attenuation by 4.8 %, from 0.041 to 0.043 M^{-1} (See eq. 10).The vertical profile of σ_t (Figure 6C) shows a large change around 100 meters. It was therefore decided to split into two linear regressions of downwelling irradiance.

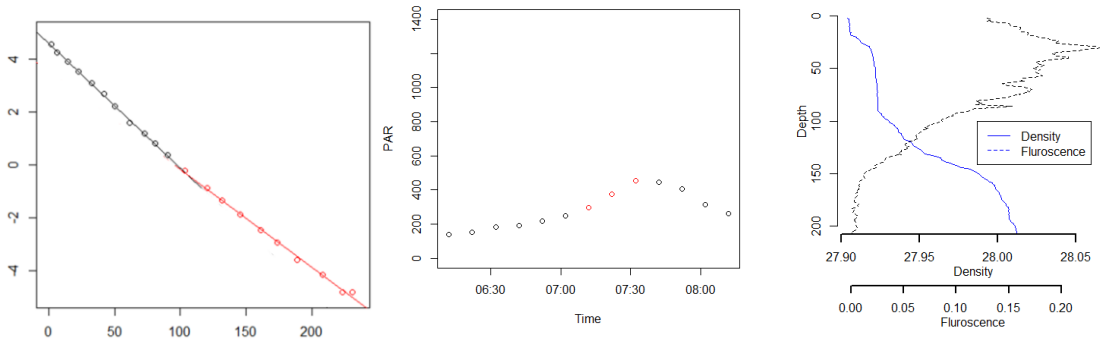

Figure 6. Left Linear regression of downwelling irradiance at Station 162, downwards. X-axis represent depth, y-axis represent downwelling irradiance. -0.0470X + 4.5959, R^2= 0.9987, SD error: : 0.0005, -0.0369X + 3.5337, R^2= 0.9969, SD error: 0.0006. Middle: Time series of PAR measurements before, during and after station 162. Red indicates PAR values during downwelling irradiance measurements. Right: σ_t and fluorescence (mg chl m^{-3}) along depth (m), at station 162.

2 Supplementary tables

Table 1. Overview of hauls from Harstad trawl and Makrozooplankton trawl along the leg. Based on 12 hauls.

Station	Trawl type	Date	Latitude	Longitude	Time	Depth (m)	Distance (Nautical miles)	Total wet weight (g)
101	Macrozooplankton trawl	05/05/2013	65 155 N	0.80 73333 W	17:24 – 18:36	310 – 290 m	2.92	3200
102	Harstad trawl	05/05/2013	65 263664 N	0.90 716666 W	19:26 – 20:27	700 – 0 m	2.39	2756
104	Macrozooplankton trawl	07/05/2013	65 66167 N	2 8930001 W	00:50 – 01:58	1028 – 0 m	2.1	942
105	Macrozooplankton trawl	07/05/2013	65 843834 N	3 9099998 W	18:39 – 18:59	500 – 500 m	0.97	2710.5
106	Macrozooplankton trawl	08/05/2013	66 72767 N	7 852667 W	11:44 – 12:30	1000 – 0 m	0.89	1740
107	Macrozooplankton trawl	09/05/2013	67 068 N	9 964833 W	10:49 – 11:19	70 – 40 m	1.32	1689
108	Macrozooplankton trawl	10/05/2013	67 6055 N	12 654333 W	10:52 – 11:22	38 – 30 m	1.37	15722
109	Harstad trawl	10/05/2013	67 668686 N	12 9365835 W	13:08 – 13:38	420 – 400 m	1.57	562
110	Harstad trawl	10/05/2013	67 70433 N	13 102333 W	14:33 – 15:03	510 – 490 m	1.56	600.6
111	Macrozooplankton trawl	11/05/2013	68 1915 N	15 401333 W	11:35 – 12:12	1000 – 0 m	1.04	2254
112	Harstad trawl	11/05/2013	68 212166 N	15 525 W	12:42 – 13:12	510 – 490 m	1.73	1143
114	Macrozooplankton trawl	11/05/2013	68 64484 N	17 675667 W	19:55 – 20:15	50 – 49 m	0.97	4916